

Role of Cdc42p in Pheromone-Stimulated Signal Transduction in *Saccharomyces cerevisiae*

JOHN J. MOSKOW,¹ AMY S. GLADFELTER,¹ RACHEL E. LAMSON,² PETER M. PRYCIAK,² AND DANIEL J. LEW^{1*}

*Department of Pharmacology and Cancer Biology, Duke University Medical Center, Durham, North Carolina 27710,¹
and Department of Molecular Genetics and Microbiology, University of Massachusetts Medical School,
Worcester, Massachusetts 01605²*

Received 13 March 2000/Returned for modification 24 April 2000/Accepted 21 July 2000

CDC42 encodes a highly conserved GTPase of the Rho family that is best known for its role in regulating cell polarity and actin organization. In addition, various studies of both yeast and mammalian cells have suggested that Cdc42p, through its interaction with p21-activated kinases (PAKs), plays a role in signaling pathways that regulate target gene transcription. However, recent studies of the yeast pheromone response pathway suggested that prior results with temperature-sensitive *cdc42* mutants were misleading and that Cdc42p and the Cdc42p-PAK interaction are not involved in signaling. To clarify this issue, we have identified and characterized novel viable pheromone-resistant *cdc42* alleles that retain the ability to perform polarity-related functions. Mutation of the Cdc42p residue Val36 or Tyr40 caused defects in pheromone signaling and in the localization of the Ste20p PAK in vivo and affected binding to the Ste20p Cdc42p-Rac interactive binding (CRIB) domain in vitro. Epistasis analysis suggested that they affect the signaling step at which Ste20p acts, and overproduction of Ste20p rescued the defect. These results suggest that Cdc42p is in fact required for pheromone response and that interaction with the PAK Ste20p is critical for that role. Furthermore, the *ste20ΔCRIB* allele, previously used to disrupt the Cdc42p-Ste20p interaction, behaved as an activated allele, largely bypassing the signaling defect of the *cdc42* mutants. Additional observations lead us to suggest that Cdc42p collaborates with the SH3-domain protein Bem1p to facilitate signal transduction, possibly by providing a cell surface scaffold that aids in the local concentration of signaling kinases, thus promoting activation of a mitogen-activated protein kinase cascade by Ste20p.

In the budding yeast *Saccharomyces cerevisiae*, cells of the α and α mating types secrete pheromones that bind to G-protein-coupled receptors on the surfaces of cells of the opposite mating type, initiating a signaling cascade in which the $\beta\gamma$ subunits of the G protein promote the activation of a mitogen-activated protein kinase (MAPK) cascade (4). This process appears to involve the binding of at least two proteins, the upstream kinase Ste20p and the scaffold protein Ste5p, to the liberated $\beta\gamma$ subunits (11, 25, 40, 51). MAPK activation then promotes cell cycle arrest in G_1 and stimulates the expression of several genes, including *FUS1*, leading ultimately to fusion of the mating partners (22).

The small GTPase Cdc42p and its guanine nucleotide exchange factor Cdc24p are essential for polarity establishment and subsequent bud formation (1, 38). In addition to their roles in cell polarity, these proteins have been proposed to play roles in signal transduction in response to mating pheromones (46, 47, 53). Temperature-sensitive *cdc42* and *cdc24* mutants have defects in α -factor-stimulated transcription of *FUS1* and in maintaining G_1 arrest at the restrictive temperature (46, 53). In addition, an interaction was detected by two-hybrid analysis between $\beta\gamma$ and Cdc24p (53), and Cdc42p-GTP was shown to bind to and activate Ste20p (46). These findings led to the hypothesis that $\beta\gamma$ activated Cdc24p, causing GTP loading of Cdc42p and consequent activation of Ste20p, as an important part of the pheromone signaling pathway.

More recent experiments have cast doubt upon the existence of a $\beta\gamma$ -Cdc24p-Cdc42p-Ste20p pathway. Mutations in

CDC24 that abolished detectable interaction with $\beta\gamma$ did not cause any defects in α -factor-stimulated *FUS1* transcription or G_1 arrest but rather were specifically defective in orientation of the mating projection towards the mating partner (33). Furthermore, mutations in *STE20* that abolished detectable interaction with Cdc42p were also reported to be wild type with regard to α -factor-stimulated *FUS1* transcription, G_1 arrest, and mating (23, 37). Together, these studies indicated that neither the $\beta\gamma$ -Cdc24p interaction nor the Cdc42p-Ste20p interaction was important for α -factor signaling. Furthermore, the polarity defect exhibited by temperature-sensitive *cdc24* and *cdc42* mutants triggers the morphogenesis checkpoint to delay the cells in G_2 with abundant G_1 cyclins (26), a state known to render cells unresponsive to α -factor (34). This raised the possibility that the signaling defect of these mutants might be an indirect consequence of their accumulation at a nonresponding stage of the cell cycle. Indeed, the transcriptional induction of *FUS1* was found to be quite normal in *cdc24* and *cdc42* mutants that were first arrested in G_1 by deprivation of G_1 cyclins (35), raising the question of whether Cdc24p and Cdc42p play any role at all in α -factor signaling.

As illustrated by these studies, the interpretation of *cdc42* and *cdc24* phenotypes is complicated by the possibility of indirect effects stemming from the well-characterized polarity defects caused by these mutants at the restrictive temperature. To circumvent these problems, we performed a screen to identify α -factor-resistant alleles of *CDC42* that could still perform polarization functions. In this paper we report the isolation and characterization of such mutants, supporting the notion that Cdc42p has some direct role in pheromone signaling. Our results further suggest that this signaling function operates through Cdc42p-dependent activation and localization of Ste20p.

* Corresponding author. Mailing address: Department of Pharmacology and Cancer Biology, Box 3686, Duke University Medical Center, Durham, NC 27710. Phone: (919) 613-8627. Fax: (919) 681-1005. E-mail: daniel.lew@duke.edu.

TABLE 1. Strains used in this study^a

Strain name	Genotype
DLY1	<i>MATa bar1</i>
DLY3067	<i>MATa bar1 cdc42::LEU2::GAL1p-CDC42</i>
MOSY0023	<i>MATa bar1 cdc42::LEU2::GAL1p-CDC42 cla4::TRP1</i>
MOSY0090	<i>MATa bar1 cdc42::URA3 leu2::GAL1p-CDC42::LEU2</i>
MOSY0095	<i>MATa bar1 cdc42::LEU2::GAL1p-CDC42</i>
MOSY0106	<i>MATa bar1 cdc42::LEU2::GAL1p-CDC42 ste20::TRP1</i>
MOSY0178	<i>MATa bar1 cdc42-md1</i>
MOSY0252	<i>MATa bar1 ste20ΔCRIB</i>
MOSY0268	<i>MATa bar1 cdc42::LEU2::GAL1p-CDC42 ste20ΔCRIB</i>
MOSY0270	<i>MATa bar1 ste20ΔCRIB bem1::URA3</i>
JMY1128	<i>MATa bar1 bem1::URA3</i>
PPY911	<i>MATa bar1 cdc42-1 FUS1::FUS1-lacZ::HIS2</i>

^a All strains are in the BF264-15Du (41a) background (*ade1 his2 leu2-3,112 trp1-1 ura3Δns*).

MATERIALS AND METHODS

Yeast media and cell synchrony. Yeast media (YEAD rich medium, synthetic complete medium lacking specific nutrients, and sporulation medium) have been described previously (13). YEPG and YEPs are the same as YEAD but with 2% galactose or sucrose instead of dextrose. Centrifugal elutriation to isolate early-G₁-phase cells was performed as described previously (27).

Strains, plasmids, and PCR manipulations. Standard media and methods were used for plasmid manipulations (2) and yeast genetic manipulations (13). The *S. cerevisiae* strains used in this study are listed in Table 1, and the plasmids used are listed in Table 2.

To generate the *GAL1p-CDC42* allele, the oligonucleotides DJL42-1 (5'-GC CGGAACCTAAAGGGTAATTCTGTAAAAACAAATCATCGACTACGT CGTAAGGCCG-3') and DJL42-2 (5'-TCAGTAGAAGGATATGACAAGG G-3') were used to amplify a DNA fragment containing the *LEU2* gene, the *GAL1* promoter, and flanking *CDC42* sequences using PCR with the plasmid pGAL-CDC42Sc (55) as a template (the underlined sequence in DJL42-1 is the genomic sequence 733 to 693 bp upstream of the *CDC42* start codon, whereas in DJL42-2 it is the reverse complement of nucleotides 204 to 226 in the *CDC42* open reading frame). The PCR fragment was transformed into DLY1, replacing the endogenous *CDC42* promoter (1 to 693 bp upstream of the start codon) with *LEU2* and the *GAL1* promoter, creating DLY3067. Leu⁺ transformants were selected on galactose-containing plates, and promoter replacement was confirmed by the inability to grow on dextrose-containing plates (*GAL1* promoter off) and by PCR.

To generate the *cdc42::URA3* null allele, the oligonucleotides CDC42-5' (5'-CTATTTCTGAGGAGATAGGTTAACAAACGAATTAGAGAAGGCCG GTTTCGGTGATGAC-3') and CDC42-3' (5'-GAGGCTCCAAGGCAGGCCA CGATAGCTCATCGAATAACATTCTTCTGATGCGGTATTTC-3') were used to amplify the *URA3* gene using PCR with the plasmid pRS306 (45) as a template. The PCR product was transformed directly into a yeast strain containing an additional copy of *CDC42* under the control of the *GAL1* promoter (in this case, integrated at *LEU2* using pDLB377, a YIp derivative of pGAL-CDC42Sc [55] generated by replacing the *Cla*I fragment containing pRS315 vector sequences with the corresponding fragment from pRS305 [45]). Ura⁺ transformants were selected on galactose-containing plates to replace the endogenous copy of *CDC42* (from 45 bp upstream to 494 bp downstream of the start codon, removing all but the last 26 codons) with *URA3*, generating strain MOSY0090. Transformants were tested for the inability to grow on dextrose-containing plates (*GAL1* promoter off), and gene replacement was confirmed by PCR.

cdc42-md1 was integrated into the endogenous *CDC42* locus by one-step replacement of the *cdc42::URA3* allele. A 1.2-kb *Eco*RI fragment containing *cdc42-md1* was excised from pMOSB36 and transformed into MOSY0090 together with the *TRP1*-marked plasmid, pRS314 (45). Trp⁺ transformants were selected on galactose-containing plates and then selected for the ability to grow on dextrose-containing plates (*GAL1* promoter off) containing 5-fluoroorotic acid (to kill *URA3* cells [7]), and gene replacement was confirmed by PCR. *cdc42-md1* was then back-crossed to separate it from the *leu2::GAL1p-CDC42::LEU2* present in MOSY0090, generating MOSY0178.

To create pDLB643, the template for PCR mutagenesis of *CDC42*, the *CDC42* promoter and coding sequences were fused to the transcription terminator sequences from *TDH3*. The oligonucleotides DJL42-3 (5'-CCACCGTCGATTCA AGGGTC-3') and DJL42-4 (5'-AGATCTGAGCAAAGCG-3') were first used to amplify *CDC42* (from 366 bp upstream of the start codon to 30 bp downstream of the stop codon) using the plasmid YEp351-CDC42 (55) as a template, and this fragment was cloned into pCR2.1 (Invitrogen, Carlsbad, Calif.) to make pCR42-3/4. The *TDH3* transcription terminator sequences (a 900-bp *Bam*HI/*Bgl*II fragment from pAB23BX [43]) were then cloned into the *Bam*HI site of pCR42-3/4 to make pDLB643. A 2-kb *Xba*I/*Bam*HI fragment

TABLE 2. Plasmids used in this study

Plasmid	Description	Reference or source
pDLB377	<i>LEU2 GAL1p-CDC42</i>	See text
pDLB642	pCR2.1 <i>CDC42p-TDH3t</i>	See text
pDLB643	pCR2.1 <i>CDC42p-CDC42-TDH3t</i>	See text
pDLB644	CEN <i>URA3 CDC42p-TDH3t</i>	See text
pDLB722	2 μ m <i>URA3 CLA4</i>	Erfei Bi
pDLB1034	pUNI-10 <i>CDC42-Q61L</i>	See text
pDLB1035	pUNI-10 <i>CDC42-D57Y</i>	See text
pDLB1160	pUNI-10 <i>CDC42-V36A,Q61L</i>	See text
pDLB1234	pHB1-MYC3 <i>CDC42-D57Y</i>	See text
pDLB1235	pHB1-MYC3 <i>CDC42-Q61L</i>	See text
pDLB1240	pHB1-MYC3 <i>CDC42-V36A,Q61L</i>	See text
pDLB1242	pHB1-MYC3 <i>CDC42-Y40C,Q61L</i>	See text
pDLB1277	pUNI-10 <i>CDC42-Y40C,Q61L</i>	See text
pG11-4	CEN <i>URA3 GAL1p-STE11-4</i>	See text
pGEX-Ste20CRIB	<i>GST-STE20-CRIB</i>	See text
pGS11ΔN-T	CEN <i>TRP1 GAL1p-GST-STE11ΔN</i>	See text
pGFP-GS5ΔN-CTM	CEN <i>TRP1 GAL1p-GFP-STE5ΔN-CTM</i>	40
pGFP-GS5ΔN-Sec22	CEN <i>TRP1 GAL1p-GFP-STE5ΔN-Sec22</i>	40
pL19	CEN <i>URA3 GAL1p-STE4</i>	50
pL-GS5ΔN-CTM	CEN <i>LEU2 GAL1p-STE5ΔN-CTM</i>	40
pMOSB16	pCR2.1 <i>cdc42-V36A</i>	See text
pMOSB29	<i>LEU2 GAL1p-CDC42-D57Y</i>	See text
pMOSB36	CEN <i>URA3 cdc42-md1</i>	See text
pMOSB37	CEN <i>URA3 cdc42-md2</i>	See text
pMOSB38	CEN <i>URA3 cdc42-md12</i>	See text
pMOSB42	CEN <i>TRP1 cdc42-md1</i>	See text
pMOSB43	CEN <i>TRP1 cdc42-md2</i>	See text
pMOSB44	CEN <i>TRP1 cdc42-md12</i>	See text
pMOSB45	CEN <i>TRP1 CDC42</i>	See text
pMOSB47	CEN <i>TRP1 cdc42-Y36A</i>	See text
pMOSB53	pCR2.1 <i>cdc42-Y40C</i>	See text
pMOSB55	CEN <i>URA3 CDC42</i>	See text
pMOSB134	<i>URA3 ste20ΔCRIB</i>	See text
pMOSB175	CEN <i>TRP1 cdc42-Y40C</i>	See text
pMOSB176	CEN <i>URA3 cdc42-Y40C</i>	See text
pMOSB177	CEN <i>URA3 cdc42-V36A</i>	See text
pNC252	2 μ m <i>URA3 GAL1p-STE12</i>	39
pPB321	2 μ m <i>URA3 BEM1</i>	5
pPP828	CEN <i>LEU2 GFP-STE20</i>	See text
pRL116	CEN <i>URA3 GFP-STE20</i>	23
pSB231	CEN <i>URA3 FUS1-lacZ</i>	48
pVTU-Ste20	2 μ m <i>URA3 ADH1p-STE20</i>	21
p3058	CEN <i>LEU2 FUS1p-lacZ</i>	C. Boone

from pDLB643 was also cloned into the corresponding sites of pRS316 (45) to make pMOSB55.

To create pDLB644, the recipient plasmid for expressing the mutant alleles of *CDC42*, *CDC42* promoter sequences were fused (via a unique *Bgl*II site) to the transcription terminator sequences from *TDH3* and cloned into the vector pRS316 (45). The oligonucleotides DJL42-3 (see above) and DJL42-5 (5'-AGA TCTGGAAGACCTAATACG-3'; the *Bgl*II site is underlined) were used to amplify a DNA fragment containing the *CDC42* promoter (1 to 366 bp upstream of the start codon) using the plasmid YEp351-CDC42 (55) as a template, and this fragment was cloned into pCR2.1 (Invitrogen) to make pCR42-3/5. The *TDH3* transcription terminator sequences were then cloned into the *Bam*HI site of pCR42-3/5 to create pDLB642. The 1.2-kb *Xba*I/*Bam*HI fragment from pDLB642 was then cloned into the corresponding sites of pRS316 (45) to make pDLB644. pDLB644 was linearized by digestion with *Bgl*II and transformed into yeast cells together with the mutagenized *CDC42* PCR products which underwent gap repair to yield Ura⁺ colonies.

The *cdc42-V36A*, *cdc42-Y40C*, and *cdc42-D57Y* alleles were constructed using the ExSite PCR-based site-directed mutagenesis kit (Stratagene, La Jolla, Calif.). To generate pMOSB16 (*cdc42-V36A*), PCR was performed using the oligonucleotides cdc-4 (5'-ACAGCGTTGATAACTATGCGG-3') and cdc-11 (5'-TG GAACATAGTCAGCTGGAAATTGATTGCG-3') with pDLB643 as a template. cdc-11 has a silent mutation which introduces a *Pvu*II site (underlined). To generate pMOSB53 (*cdc42-Y40C*), PCR was performed using the oligonucleotides cdc-22 (5'-ACAGTGTGAGATAACTGTGCGGTGACTGTGATG-3') and cdc-11 with pDLB643 as a template. To generate pMOSB29 (*cdc42-D57Y*),

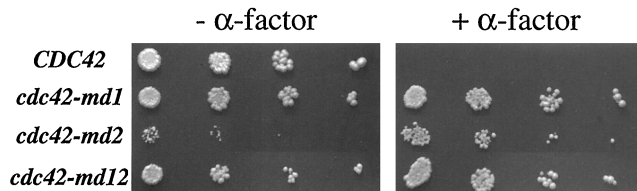


FIG. 1. Isolation of α -factor-resistant *cdc42* alleles. The results of growth arrest assays of strain DLY3067 (*GAL1p-CDC42*) containing plasmid pMOSB55 (*CDC42*), pMOSB36 (*cdc42-md1*), pMOSB37 (*cdc42-md2*), or pMOSB38 (*cdc42-md12*) are shown. The photographs show growth after 3 days at 30°C with (+) or without (-) α -factor.

PCR was performed using the oligonucleotides *cdc*-18 (5'-TATACGGCCGGT CAAGAAG-3') and *cdc*-19 (5'-AAACAAACCTAACGTATATGG-3') with pDLB377 as a template. The mutants were sequenced to confirm the presence of the desired mutation and the absence of any other mutations.

To generate pMOSB176 and pMOSB177, PCR was performed using the oligonucleotides DJL42-3 (see above) and DJL42-6 (5'-CTACTACAGATTAT ACATGTGGCG-3') to amplify *cdc42-Y40C* (pMOSB53 template) or *cdc42-V36A* (pMOSB16 template), respectively, and introduced into pDLB644 by gap repair. To generate pMOSB175 and pMOSB47, 2.1-kb *Bam*H/*Xba*I fragments containing *cdc42* alleles were excised from pMOSB176 and pMOSB177, respectively, and cloned into the corresponding sites of pRS314 (45).

The *cdc42-V36A*, *Q61L* and *cdc42-Y40C*, *Q61L* alleles were generated by a two-step strategy in which we first removed residues 32 to 40 in *CDC42-Q61L* and then employed homologous recombination to repair that "gap" with sequences from *cdc42-V36A* or *cdc42-Y40C*. We first replaced amino acids 32 to 40 in *CDC42-Q61L*, *C188S* with a *NoI* site, using the ExSite PCR-based site-directed mutagenesis kit. PCR was performed with the oligonucleotides JMCDC42-1 (5'-C CGCGTCGGCTGAAATTGATTG-3') and JMCDC42-2 (5'-CCGCGGTG ACTGTGATGATTGG-3') with pEG202-*cde42-Q61L*, *C188S* (46) as a template. The resulting allele was then transferred to pOBD.CYH using a PCR and gap repair strategy involving sequential amplification of the allele with the oligonucleotides LC20-*CDC42* (5'-AATTCCAGCTGACCACCATGCAAACG CTAAAGTGTG-3') and RC20-*CDC42* (5'-GATCCCCGGGAATTGCCATG CTACAAAATTGATGATTG-3') followed by a second PCR using the oligonucleotides BD70F and BD70R (15) containing homology to the first primers and 70-nucleotide extensions with homology to pOBD.CYH. The resulting PCR product was transformed together with *Pvu*II/*Nco*I-linearized pOBD.CYH into DLY1 to generate pOBD.CYH-*cde42-Q61L*/*C188S*(A32-40) by gap repair. *cdc42-V36A* and *cdc42-Y40C* were then amplified by PCR using the oligonucleotides DJL42-3 and *cdc*-19 (see above) with pMOSB16 or pMOSB53 as a template and transformed into DLY1 together with *NoI*-cut pOBD.CYH-*cde42-Q61L*/*C188S*(A32-40) to generate the gap repair products pOBD.CYH-*cde42-V36A*/*Q61L*/*C188S* and pOBD.CYH-*cde42-Y40C*/*Q61L*/*C188S*.

Plasmids for the expression of myc-tagged alleles of *CDC42* in bacteria were made using the Univector system (28). *CDC42* alleles were amplified by PCR using the oligonucleotides *CDC42-UNI1* (5'-GGAATTCCATATGCAACACG TAAAGTGTGTTGTC-3'; the *Nde*I site is underlined, and the start codon is in boldface) and *CDC42-UNI2* (5'-CCGAGCTCCTACAAATTGTACATT TTAACTTTTC-3'; the *Sac*I site is underlined) with pGAL-*CDC42(Q61L)* (55), pMOSB29, pOBD.CYH-*cde42-V36A*/*Q61L*/*C188S*, or pOBD.CYH-*cde42-Y40C*/*Q61L*/*C188S* as a template. *Nde*I/*Sac*I-digested PCR fragments were cloned into the respective sites of pUNI-10 (28), generating pDLB1034, -1035, -1160, and -1277. The pUNI-10-*CDC42* plasmids were then recombined with pHB1-MYC3 using the Cre/lox system (28) to produce the bacterial expression plasmids pDLB1234, -1235, -1240, and -1242. All constructs were sequenced to confirm that no changes occurred as a result of PCR manipulations.

To construct pG11-4, *STE11-4* was amplified by PCR and inserted downstream of the *GAL1p* promoter in pRD53* as a *Bam*H/*Xba*I fragment; pRD53* is a derivative of pRD53 (40) in which *URA3* lacks a *Pst*I site.

Plasmid pGS11ΔN-T was constructed by transferring the 3.5-kb *Sac*I/*Xba*I fragment encoding *GAL1p-GST-STE11ΔN* from pRD-*STE11-H3* (32) into the corresponding sites in pRS314 (45).

Plasmid pPP828 is a *LEU2*-marked derivative of pRL116 (23) created by homologous recombination in yeast using pUC4-ura3::*LEU2* (31).

To express the Ste20p Cdc42p-Rac interactive binding (CRIB) domain as a recombinant glutathione S-transferase (GST) fusion protein, the oligonucleotides ste20-1 (5'-ATGTCATCTCTATAACCACCGC-3') and ste20-2 (5'-TGT TTGCAGCGGTGTTG-3') were used to amplify a DNA fragment encoding the Ste20p residues 328 to 428 by PCR using yeast genomic DNA as a template. The PCR fragment was cloned into pCR2.1 using the TA cloning kit (Invitrogen) and then excised using the flanking *Eco*RI sites and cloned into the *Eco*RI site of pGEX-KG, generating pGEX-Ste20CRIB. The construct was sequenced to confirm its orientation and that no PCR-induced mutations had occurred.

To generate the *ste20ΔCRIB* allele (23), the 3-kb *Sph*I/*Kpn*I fragment from

pRS316-*ste20*(Δ334-369) (23) was cloned into the corresponding sites of *YI-plac211* (12), generating pMOSB134. pMOSB134 was digested at the unique *Xba*I site within *STE20* (upstream of the deleted CRIB region) and transformed into DLY3067. *Ura*⁺ transformants containing tandem *STE20-URA3-ste20ΔCRIB* sequences were selected, and then "pop-out" events in which *URA3*-containing sequences between the *STE20* and *ste20ΔCRIB* genes were excised by homologous recombination were selected by plating them on 5-fluoroorotic acid. The colonies were screened by PCR using the oligonucleotide *ste20-2* (5'-GAGTTT GCAGCGGTGTTG-3') and *ste20-9* (5'-AACCGTCCAAGCTCTGAAG-3') to determine whether the excision event left *STE20* (558-bp PCR product) or *ste20ΔCRIB* (446-bp PCR product) as the sole remaining allele.

Strains MOSY0023 and MOSY0106 were generated from a cross between MOSY0095 and BOY774 (*cla4::TRP1*) or BOY489 (*ste20::TRP1*), respectively. BOY489 and BOY774 were obtained from F. Cross (6).

The *bem1::URA3* allele was generated by one-step gene replacement using an *Eco*RI-*Bam*H fragment from the plasmid pKO1 (9).

Strain PPY911 (40) contains a *HIS2*-marked *FUS1-lacZ* reporter integrated at the *FUS1* locus that was introduced by transformation of the *cde42-1* strain DLY3032 with *Sph*I-digested pFL-HIS2. pFL-HIS2 contains a 2-kb *HIS2* *Hind*III fragment in place of the *Hind*III/*Hind*III *TRP1* fragment in pFL-TRP2, which itself contains a 0.9-kb *TRP1* *Eco*RI/*Stu*I fragment (along with pBluescript polylinker sequences from *Eco*RI/*Hinc*II) in place of the *Hind*III/*Stu*I *URA3* fragment of pSB286 (39).

Screen to identify α -factor-resistant *cde42* mutants. The oligonucleotides DJL42-3 and DJL42-6 (see above) were used to amplify *CDC42* (and *TDH3* terminator sequences) by mutagenic PCR using pDLB643 as a template. Mutagenic PCRs were similar to standard PCR except for the addition of 0.2 mM MnCl₂ and the use of an unbalanced deoxynucleoside triphosphate mix (0.5 mM dTTP, 0.5 mM dGTP, 0.1 mM dATP, and 0.1 mM dCTP [final concentrations]). The PCR products were transformed into DLY3067 together with *Bgl*II-digested ("gapped" plasmid) pDLB644, and *Ura*⁺ transformants were selected on dextrose-containing plates (to repress transcription of the genomic *GAL1p-CDC42* allele) coated with 10 μ g of α -factor (to select for α -factor-resistant *cde42* mutants). This amount of α -factor (custom synthesized by Research Genetics, Huntsville, Ala.) was more than 10 times the amount needed to completely inhibit growth of the *bar1* parent strain. α -Factor-resistant colonies could in theory arise due to genomic mutations in other genes. To distinguish *cde42* mutants, colonies were tested for α -factor-resistant growth on galactose-containing plates, where the genomic (wild-type) *CDC42* is expressed. Plasmids were isolated from colonies that were α -factor resistant when grown in dextrose-containing medium but not when grown in galactose-containing medium and were then retransformed into fresh DLY3067 to confirm that the plasmids were responsible for the α -factor-resistant growth phenotype. To generate the *TRP1*-containing plasmids pMOSB42 to -45, *CDC42* alleles were transferred from *URA3* plasmids (pMOSB36 to -38 and pMOSB55) as 2.1-kb *Bam*H/*Xba*I fragments to the corresponding sites of pRS314 (45).

Spot assays for growth arrest. Cells harboring plasmid-borne *CDC42* alleles were grown to stationary phase in dextrose-containing medium (to repress genomic *GAL1p-CDC42*) lacking nutrients appropriate to select for plasmid maintenance. The number of cells was determined using a hemocytometer, and diluted stocks were generated to spot 2 μ l containing ~1,250, ~250, ~50, and ~10 cells onto plates containing the same selective dextrose medium either with or without 10 μ g of α -factor per plate. Assuming a plate "volume" of 20 ml, this would translate to ~0.3 μ M α -factor.

Northern blot analysis. RNA extraction, formaldehyde-agarose gel electrophoresis, capillary transfer, probe hybridization, and wash procedures were performed as described previously (10, 41, 42). The *FUS1* probe was made from a 880-bp internal *Eco*RI/*Nhe*I fragment from the *FUS1* gene, and the *ACT1* probe was made from the entire *ACT1* open reading frame, using [α -³²P]dCTP (ICN Pharmaceuticals, Costa Mesa, Calif.) and the Prime-it II kit (Stratagene) according to the manufacturer's recommendations.

Flow cytometry. Cells were processed for fluorescence-activated cell sorter (FACS) analysis as described (14), except that the DNA was stained with 1 μ M Sytox (Molecular Probes, Eugene, Oreg.) in 50 mM Tris-HCl (pH 8.0) (instead of propidium iodide).

DIC microscopy. Cells were viewed on an Axioskop apparatus (Zeiss, Thornwood, N.Y.) equipped with epifluorescence and differential interference contrast (DIC) optics. Images were captured by using a cooled-model charge-coupled device camera (Princeton Instruments, Princeton, N.J.).

Analysis of *FUS1-lacZ* expression. β -Galactosidase assays were performed as described previously (40). Transformants in *cde42-1* strains were grown overnight at 28°C in selective synthetic medium containing 2% raffinose and 0.1% dextrose to an optical density at 660 nm of 0.3 to 0.6, preincubated for 2 h at 38.5°C, and then induced for 4 h with 2% galactose with or without 0.01 μ M α -factor. Assays in *CDC42* strains were performed at 30°C.

Production of recombinant proteins and binding assays. Wild-type and mutant myc-tagged *CDC42* alleles were expressed in *Escherichia coli* BL21(DE3) (Stratagene). Extracts were prepared in bacterial lysis buffer (750 mM sucrose, 100 mM NaCl, 100 mM Tris-HCl [pH 8.0], 5 mM EDTA) containing the protease inhibitors aprotinin (7.5 μ g/ml; Sigma, St. Louis, Mo.), pepstatin (5 μ g/ml; Sigma), leupeptin (10 μ g/ml; Boehringer Mannheim, Indianapolis, Ind.), and phenylmethylsulfonyl fluoride (0.5 mM; Sigma). The cells were treated with 2 mg

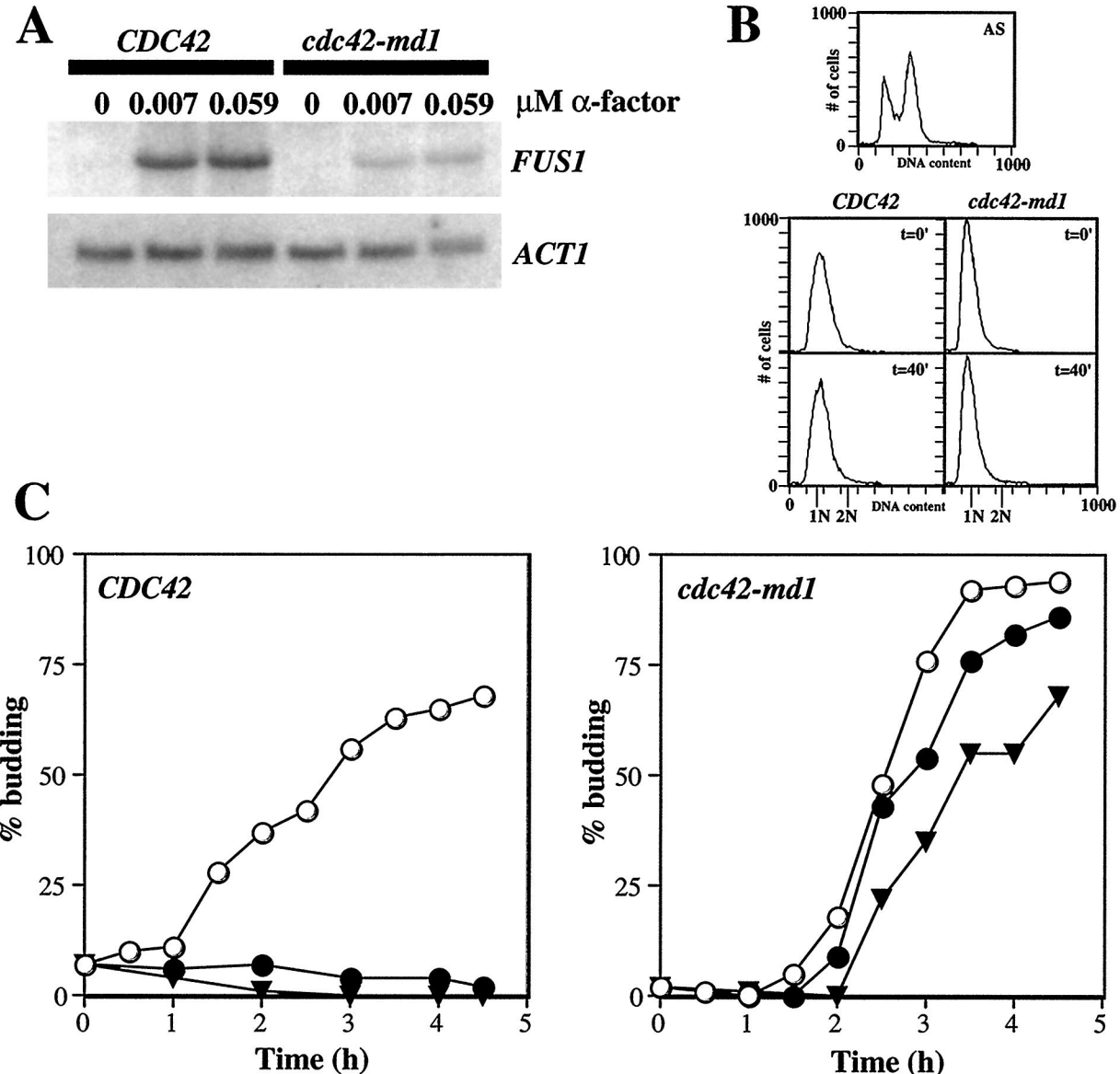


FIG. 2. *FUS1* induction and cell cycle arrest in early-G₁-phase cells. Cells containing two copies of wild-type *CDC42* (DLY1 plus pMOSB55) or *cdc42-md1* (MOSY0178 plus pMOSB36) were grown to exponential phase in sucrose-containing medium lacking uracil at 30°C (using two gene copies improved the morphology of *cdc42-md1* cells, making the elutriation more effective). Small G₁-phase cells were isolated by centrifugal elutriation and resuspended in YEPD medium at 30°C. Following a 10-min recovery period, α-factor was added to the indicated final concentrations and the incubation was continued with vigorous shaking. (A) Northern blot of *FUS1* mRNA accumulation following 30 min of α-factor treatment. *cdc42-md1* cells display severely reduced induction compared to wild-type cells. *ACT1* mRNA on the same blots provides an internal control for loading and transfer. (B) FACS analysis demonstrating that both wild-type and *cdc42-md1* cells were still in G₁ phase after 40 min in YEPD medium without α-factor (the same time point used for the *FUS1* mRNA analysis; a 10-min recovery period plus a 30-min α-factor treatment). The FACS profile of asynchronous wild-type cells (top) was used to determine the fluorescence signal equivalent to G₁ (1 N) and G₂ (2 N) DNA content. FACS profiles are shown for the indicated strains immediately following elutriation (t = 0') or 40 min later in the absence of α-factor (t = 40'). (C) *cdc42-md1* cells were not arrested in G₁ phase in response to α-factor. Aliquots of cells were withdrawn at the indicated times, fixed, and examined by phase-contrast microscopy to determine the percentage of budded cells ($n = 200$). ○, no α-factor; ●, 0.015 μM α-factor; ▼, 0.059 μM α-factor.

of lysozyme/ml for 20 min on ice. To remove genomic DNA, MgCl₂ was added to 15 mM and DNase I was added to 50 μg/ml. The cells were lysed by 20 min of incubation at 4°C with 2 mg of deoxycholic acid/ml. Insoluble material was removed by centrifugation at 4°C for 10 min. GST-Ste20-CRIB was expressed in the protease-deficient *E. coli* BL21, extracts were prepared as described above, and the protein was purified using glutathione Sepharose 4B (Amersham Pharmacia Biotech, Piscataway, N.J.) as specified by the manufacturer.

Binding assays were performed by incubating the bacterial extracts containing Cdc42p-myc with either GST or GST-Ste20-CRIB immobilized on glutathione beads in 200 μl of binding buffer (10 mM Tris-HCl [pH 7.5], 85 mM NaCl, 6 mM MgCl₂, 10% glycerol) at 4°C for 3 h. Binding reaction mixtures were washed three times at room temperature with wash buffer (10 mM Tris-HCl [pH 7.5], 10

mM MgCl₂, 1 mM dithiothreitol, 0.1% Triton X-100). Bead-bound proteins were resolved by sodium dodecyl sulfate-polyacrylamide gel electrophoresis, blotted to Immobilon-P nylon membranes (Millipore, Bedford, Mass.), and immunoblotted with monoclonal anti-myc antibodies (9E10; Santa Cruz Biotechnology, Santa Cruz, Calif.) using standard procedures (2). To confirm equal loading, the amount of GST-Ste20-CRIB in each lane was visualized by staining the membrane with India ink (42).

Localization of GFP-Ste20p. Cells containing pRL116 or pPP828 were propagated for at least 24 h in selective liquid medium containing 2% dextrose and 0.008% adenine (to inhibit accumulation of red pigment in *ade1* cells) at 30°C (*GAL1p-CDC42* strains) or at 36°C (*cdc42-1* strains). The cells were examined without fixation using a Nikon E600 epifluorescence microscope with 100× Plan

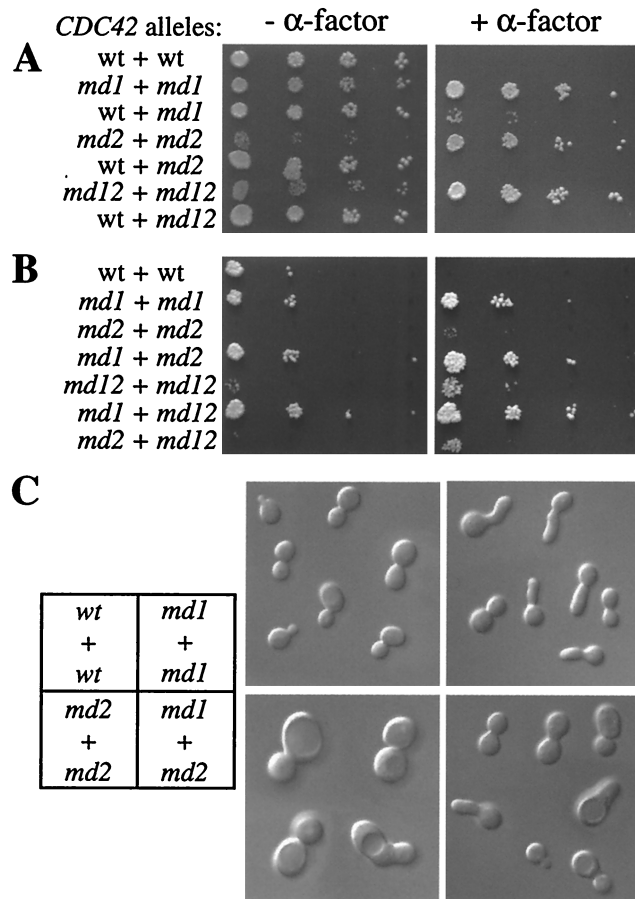


FIG. 3. Intragenic-complementation analysis of the *cdc42-md* mutants. Plasmids containing the indicated pairs of *CD42* alleles were transformed into strain DLY3067. (A) Pheromone resistance of *cdc42-md* mutants is recessive. The photographs show growth after 3 days at 30°C with (+) and without (-) α-factor. The plasmid pairs were (in order) pMOSB55 plus pMOSB45, pMOSB36 plus pMOSB42, pMOSB55 plus pMOSB42, pMOSB37 plus pMOSB43, pMOSB55 plus pMOSB43, pMOSB38 plus pMOSB44, and pMOSB55 plus pMOSB44. wt, wild type. (B) *cdc42-md* mutants form a single complementation group with regard to α-factor resistance. Spot assays were performed as for panel A (except that fewer cells were spotted in this experiment). The plasmid pairs were (in order) pMOSB55 plus pMOSB45, pMOSB36 plus pMOSB42, pMOSB37 plus pMOSB43, pMOSB36 plus pMOSB43, pMOSB38 plus pMOSB44, pMOSB36 plus pMOSB44, and pMOSB37 plus pMOSB44. (C) *cdc42-md* mutants form two complementation groups with regard to cell morphology. Cells were grown to exponential phase and photographed using DIC optics. *cdc42-md1* mutants exhibit broad necks and elongated buds (48% of cells), while *cdc42-md2* mutants exhibit large round cells (>70% of cells); although some abnormal cells are present in the *cdc42-md1* plus *cdc42-md2* population (with generally less severe defects, perhaps due to plasmid loss), the majority (73%) exhibit normal morphology. The morphologies were similar in the presence and absence of α-factor. The plasmid pairs were pMOSB55 plus pMOSB45 (wt + wt), pMOSB36 plus pMOSB42 (*md1* + *md1*), pMOSB37 plus pMOSB43 (*md2* + *md2*), and pMOSB36 plus pMOSB43 (*md1* + *md2*).

Fluor and 50× Plan oil-immersion objectives. Images were collected using a cooled black and white charge-coupled device camera (DAGE-MTI).

RESULTS

Identification of recessive α-factor-resistant alleles of *CDC42*. A hypothetical *cdc42* mutant specifically defective in pheromone signal transduction should retain all functions necessary for cell polarity and proliferation but would fail to arrest in G₁ upon exposure to α-factor. Thus, cells expressing such an allele as the sole source of Cdc42p should proliferate and form

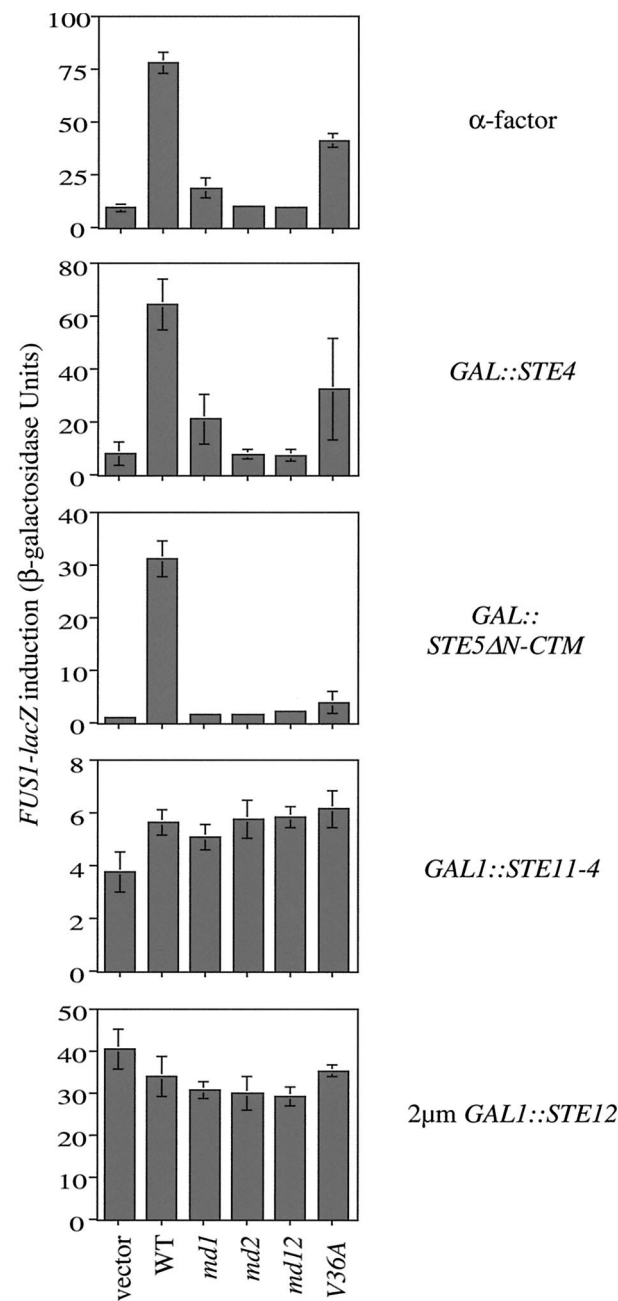


FIG. 4. Epistasis analysis of *cdc42-md* mutants. Strain PPY911 (*cdc42-1*) was transformed with pRS314 (vector), pMOSB45 (wild type [WT]), pMOSB42 (*md1*), pMOSB43 (*md2*), pMOSB44 (*md12*), or pMOSB47 (V36A), as indicated. Each of these strains was then transformed with the mating-pathway-activating plasmids pL19 (*GAL1p-STE4* [*GAL::STE4*]), pL-GS5ΔN-CTM (*GAL1p-STE5ΔN-CTM* [*GAL::STE5ΔN-CTM*]), pG11-4 (*GAL1p-STE11-4* [*GAL1::STE11-4*]), or pNC252 (2μm *GAL1p-STE12* [2μm *GAL1::STE12*]) as indicated on the right. Transformants grown at restrictive temperature to inactivate *cdc42-1* were induced with 2% galactose (or 2% galactose plus 0.01 μM α-factor; top). The bars indicate the means ± standard deviation for four to six independent transformants. Results similar to those shown with *STE5ΔN-CTM* were also seen with *STE5-CTM*, and results similar to those shown with *GAL1p-STE11-4* were also seen with *GAL1p-STE11ΔN* (data not shown).

colonies on plates containing a growth-inhibitory dose of α-factor. We employed an error-prone PCR mutagenesis strategy to generate random mutations in *CDC42* and recombined the resulting allele into a low-copy-number plasmid in cells whose

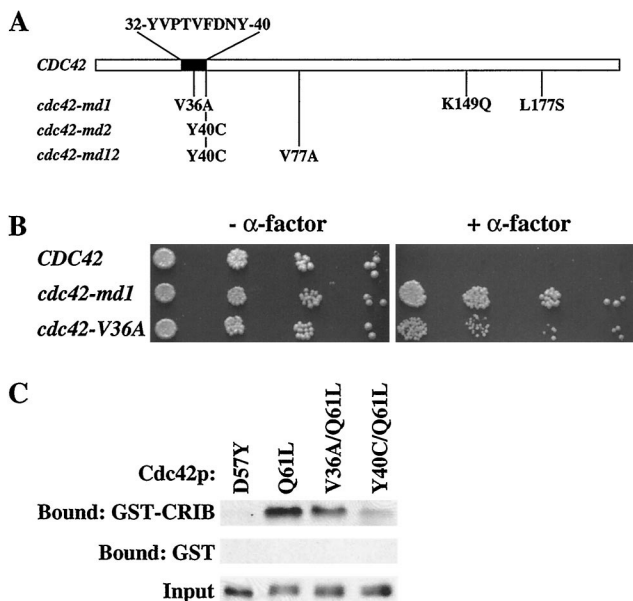


FIG. 5. Defective interaction of *cdc42-md* mutants with Ste20p. (A) Altered residues in *cdc42-md* mutants. (B) The V36A substitution confers α-factor resistance. Growth arrest assays of strain DLY3067 (*GAL1p-CDC42*) containing plasmid pMOSB55 (*CDC42*), pMOSB36 (*cdc42-md1*), or pMOSB177 (*cdc42-V36A*) were performed. The photographs show growth after 3 days at 30°C with (+) or without (−) α-factor. (C) Binding of *cdc42* mutants to the Ste20p CRIB domain. The binding conditions were as described in Materials and Methods. The top row shows the amount of the indicated myc-tagged Cdc42p mutant that bound to immobilized GST-CRIB, the second row shows the amount of each Cdc42p mutant that bound to immobilized GST (to control for nonspecific adsorption), and the third row shows the amount of each Cdc42p mutant added to the binding reaction. India ink staining of the blots confirmed that equal amounts of GST or GST-CRIB were present in each lane. Similar results were obtained in four independent experiments. Recombinant Cdc42p was generated from pDLB1234 (D57Y, mimicking GDP-bound Cdc42p), pDLB1235 (Q61L, mimicking GTP-bound Cdc42p), pDLB1240 (V36A and Q61L), or pDLB1242 (Y40C and Q61L).

endogenous *CDC42* was transcriptionally repressed (using the regulatable *GAL1* promoter; see Materials and Methods for details). Transformants that promoted proliferation on α-factor-containing plates were selected. Plasmids containing putative *CDC42* mutants were isolated from the rare α-factor-resistant colonies and retransformed into the starting strain to confirm that the α-factor resistance was due to the plasmid and not to a fortuitous genomic mutation. Three independently derived mutants (*cdc42-md1*, *cdc42-md2*, and *cdc42-md12* [*md* for mating pathway defective]) were selected for further characterization (Fig. 1).

In addition to promoting growth on α-factor-containing plates (Fig. 1), strains bearing the *cdc42-md* alleles were significantly, though not completely, defective in α-factor-induced *FUS1* transcription (see below) and in mating to a wild-type partner (data not shown). A possible explanation for the defect in *FUS1* induction observed previously in temperature-sensitive *cdc42* mutants is that the mutants accumulate at a nonresponding stage (post-*G₁*) of the cell cycle (35). To address whether a similar situation might apply with *cdc42-md* mutants, we isolated early-*G₁*-phase cells from *cdc42-md1* and isogenic wild-type strains using centrifugal elutriation and monitored cell cycle progression and *FUS1* mRNA accumulation upon treatment with different doses of α-factor. As shown in Fig. 2A, *cdc42-md1* cells synchronized in early *G₁* phase displayed a defect in *FUS1* induction compared to similarly treated wild-type cells, suggesting that these mutants are de-

fective in responding to α-factor even when the cells are in a responsive stage of the cell cycle. Flow cytometric analysis confirmed that both mutant and wild-type cells remained in *G₁* for the duration of the 30-min α-factor treatment (Fig. 2B). In addition, *cdc42-md1* mutants progressed into S phase (data not shown) and formed buds (Fig. 2C) with unaltered kinetics in the continuous presence of 0.015 μM α-factor, a concentration sufficient to completely arrest wild-type cells. However, 0.06 μM α-factor did cause *cdc42-md1* cells to delay briefly in *G₁* (Fig. 2C), indicating that the signaling defect is not complete (consistent with the *FUS1* induction data). In other experiments, we have found that *cdc42-md* mutants also show a *FUS1* induction defect in cells arrested in *G₁* by depletion of the *G₁* cyclins Cln1p-Cln3p (data not shown). Together, these data strongly suggest that the signaling defect of *cdc42-md* mutants is not due to arrest at a nonresponding stage of the cell cycle.

In principle, the *cdc42-md* mutants could be defective for a normal function of Cdc42p in α-factor signaling or they could encode forms of Cdc42p that can interfere with α-factor signaling even though wild-type Cdc42p might not play a role in signaling. To distinguish between these options, we performed a dominance test to determine whether cells containing both wild-type and mutant forms of *CDC42* were α-factor resistant. As shown in Fig. 3A, the mutants were all recessive, in that cells containing plasmids expressing both wild-type and mutant Cdc42p were α-factor sensitive. Intriguingly, very tiny colonies were reproducibly observed in strains containing both *cdc42-md1*- and *CDC42*-expressing plasmids. This appears to be a dose-dependent effect such that cells with a high *cdc42-md1/CDC42* plasmid ratio are selected for on α-factor plates: when this experiment was repeated in cells with an integrated copy of *cdc42-md1* and a plasmid-borne copy of *CDC42*, no pheromone-resistant growth was observed (data not shown). The recessive behavior of these alleles suggests that Cdc42p wild-type function is required for an efficient pheromone response.

Intragenic complementation analysis of the *cdc42-md* mutants. We took advantage of the recessive nature of these alleles to determine whether they had defects in the same or different functions required for the α-factor response. Cells containing all pairwise combinations of plasmids bearing different *cdc42-md* alleles were uniformly resistant to α-factor (Fig. 3B), indicating that no mutant could provide the signaling function(s) defective in another and suggesting that all three alleles were defective for the same function.

In addition to the α-factor-resistant phenotype, two of the mutants (*cdc42-md2* and *cdc42-md12*) displayed a slow-growth phenotype (Fig. 1A and 3A) (interestingly, growth of these mutants was actually stimulated by α-factor), and all three mutants displayed aberrant cell morphologies when grown in the absence of α-factor (Fig. 3C) (a detailed analysis of the morphological phenotypes will be presented elsewhere). Like α-factor resistance, the slow growth and morphological phenotypes were recessive (Fig. 3A and data not shown). However, cells containing two plasmids expressing *cdc42-md1* and *cdc42-md2* or *cdc42-md1* and *cdc42-md12* but not *cdc42-md2* and *cdc42-md12* grew at wild-type rates and did not display morphological abnormalities (Fig. 3B and C and data not shown). This suggests that *cdc42-md2* and *cdc42-md12* share similar defects in vegetative growth while *cdc42-md1* has a distinct defect: in cells containing both *cdc42-md1* and *cdc42-md2*, or *cdc42-md1* and *cdc42-md12*, all vegetative functions are provided by one of the alleles and cells grow normally. This finding of intragenic complementation for the vegetative-growth defects is in contrast to the lack of such complementation for the pheromone signaling defect (Fig. 3B), suggesting

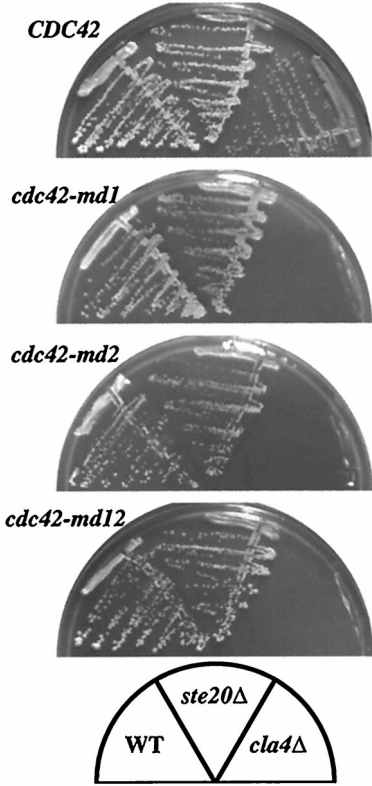


FIG. 6. Synthetic lethality of *cdc42-md* mutants with *cla4Δ* but not *ste20Δ* mutants. Strains DLY3067 (*GAL1p-CDC42*; left), MOSY0106 (*GAL1p-CDC42 ste20Δ*; middle), and MOSY0023 (*GAL1p-CDC42 cla4Δ*; right) were transformed with pMOSB55 (*CDC42*), pMOSB36 (*cdc42-md1*), pMOSB37 (*cdc42-md2*), or pMOSB38 (*cdc42-md12*), as indicated. Cells were streaked out on dextrose-containing plates (to repress the genomic *GAL1p-CDC42*) lacking uracil (to select for plasmid maintenance) and incubated at 30°C for 3 days. WT, wild type.

that the pheromone signaling defect is distinct from the vegetative-growth defects and cannot be explained as an indirect result of such defects.

Epistasis analysis of the *cdc42-md* mutants. To determine where in the pheromone response pathway Cdc42p plays a role, we examined whether the *cdc42-md* mutants could block signaling that was initiated at various steps in the pathway. Induction of a *FUS1-LacZ* reporter construct was used as a readout of pathway activation. Like signaling induced by α-factor, the signals initiated by overexpression of the Gβ subunit Ste4p, or by a membrane-targeted Ste5p scaffold protein, were substantially blocked by *cdc42-md* mutants (Fig. 4). In contrast, signals initiated by the activated MEKK gene allele *STE11-4* or by overexpression of the transcription factor Ste12p were unaffected by *cdc42-md* mutants (Fig. 4). This suggests that Cdc42p is required after Ste5p membrane recruitment for the activation of Ste11p. Previous studies have shown that this is precisely the step at which Ste20p is required (40).

Sequence analysis of *cdc42* mutants. To determine the natures of the mutations that rendered *CDC42* signaling defective, we recovered the mutant plasmids from yeast and sequenced the open reading frame of each mutant. As shown in Fig. 5A, all three mutants contained single-amino-acid changes in the “effector” domain of Cdc24p: a valine-to-alanine substitution at residue 36 in *cdc42-md1* and a tyrosine-to-cysteine substitution at position 40 in both *cdc42-md2* and *cdc42-md12*. In addition, *cdc42-md1* contained substitutions at residues 149

and 177, and *cdc42-md12* contained a valine-to-alanine substitution at residue 77 (Fig. 5A). Because the Y40C substitution was the only change in *cdc42-md2*, we assume that the α-factor resistance of *cdc42-md12* also derives from this same change. Presumably the V77A mutation confers the somewhat-improved growth properties observed in *cdc42-md12* compared to those of *cdc42-md2*. In a recent study, *cdc42^{Y40C}* was reported to be nonviable (18). The discrepancy appears to be due to the fact that in our case the mutant is expressed from a low-copy-number (CEN ARS) plasmid while in that study it was integrated into the genome. To determine which changes were responsible for the α-factor resistance of the *cdc42-md1* mutant, we constructed a mutant that contained only the V36A substitution. This mutant also conferred an α-factor-resistant phenotype (although not as strong as that conferred by *cdc42-md1* [Fig. 4 and 5B]). We conclude that a mutation at either V36 (to A) or Y40 (to C) in the effector domain of Cdc42p renders the protein signaling defective.

Defective interaction of Ste20p with *cdc42-md* mutants. The Y40C mutation has been described in human *CDC42* (which is 80% identical to yeast *CDC42* and complements a *cdc42* null mutation in yeast [44]), where it was found to render Cdc42p defective in binding to and activating p21-activated kinase (PAK), a mammalian Ste20p homologue (19). Combined with epistasis analysis (Fig. 4), this suggested that the *cdc42-md* mutants might be defective in binding to Ste20p. Binding of PAK family kinases to Cdc42p is mediated by the CRIB domain in these proteins (8). We produced the Ste20p CRIB domain as a GST fusion protein in *E. coli* and purified it using glutathione Sepharose beads. The wild type or V36A or Y40C mutants of Cdc42p were produced as myc-tagged proteins in *E. coli* and tested for binding to the GST-Ste20p-CRIB beads or to GST beads as a negative control. A Q61L substitution, which inhibits Cdc42p GTPase activity, was also engineered into the constructs to ensure that the proteins were GTP bound (a prerequisite for CRIB domain binding). As shown in Fig. 5C, the V36A substitution conferred a mild defect in Ste20p binding while the Y40C substitution conferred a severe defect.

Ste20p shares a redundant essential function with the related PAK-family kinase Cla4p. The Cdc42p-Ste20p interaction has been reported to be critical for this function (23, 37). We found that cells containing *cdc42-md* mutants as the only source of Cdc42p were synthetically lethal with *cla4Δ* mutants (but not with *ste20Δ* mutants [Fig. 6]), suggesting that these mutants fail to interact with Ste20p *in vivo* as well as *in vitro*.

Defective localization of Ste20p in *cdc42-md* mutants. Ste20p is concentrated at the bud tips of many cells during vegetative growth, and at the shmoo tips of cells responding to α-factor, in a manner that depends to a large extent on the CRIB domain (23, 37). GFP-Ste20p localization to bud tips was greatly reduced in all of the *cdc42-md* mutants (Fig. 7). Even cells containing both *cdc42-md1* and *cdc42-md2*, which exhibited a wild-type growth rate and cell morphology, failed to localize GFP-Ste20p to the bud tip in most cells (see Fig. 11 below). We were unable to address the question of whether shmoo tip localization was affected because these cells were resistant to α-factor and did not make shmoos.

Suppression of the *cdc42-md* signaling defect by overexpression of Ste20p. If the α-factor resistance phenotype of the *cdc42-md* mutants is due to defective interaction with Ste20p, then overexpression of Ste20p might suppress that phenotype. Indeed, overexpression of *STE20* substantially suppressed the α-factor-resistant growth of *cdc42-md* mutants (Fig. 8). In contrast, overexpression of the related *CLA4* did not suppress the *cdc42-md* signaling defect, although it did suppress the growth defect of *cdc42-md2* mutants in the absence of α-factor (Fig.

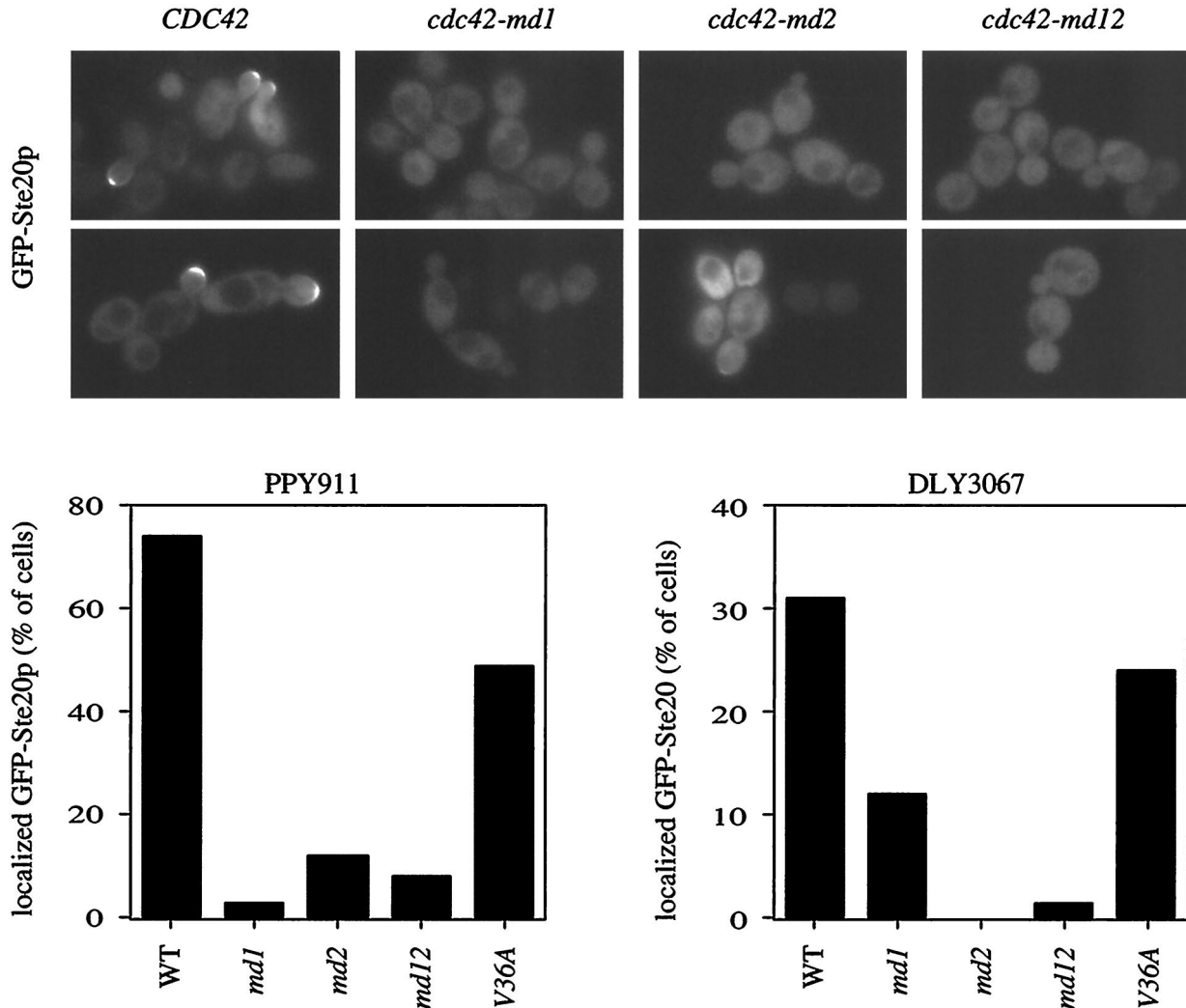


FIG. 7. Ste20p localization in *cdc42-md* mutants. Strain PPY911 (*cdc42-1*) was transformed with pRL116 (GFP-STE20 [GFP-Ste20p]) and then with pMOSB45 (*CDC45*), pMOSB42 (*cdc42-md1*), pMOSB43 (*cdc42-md2*), pMOSB44 (*cdc42-md12*), or pMOSB47 (*cdc42-V36A*) as indicated. The cells were grown at 36°C to inactivate *cdc42-1*, and the localization of GFP-Ste20p was examined by fluorescence microscopy of living cells. Representative fields are shown (top), and the percentage of budded cells displaying GFP-Ste20p concentrated at the bud tips is quantitated (bottom left). The same set of plasmids was transformed into DLY3067 (*GAL1p-CDC42*), and the cells were grown on dextrose (to repress *GAL1p-CDC42*) and analyzed as above (bottom right). Several images were captured for each transformant, and all cells within those images were scored for whether GFP-Ste20 was detectably concentrated at the bud tip. $n = 80$ to 138 (PPY911 transformants) or $n = 55$ to 91 (DLY3067 transformants).

8). These findings could be accommodated by at least two models: the observed suppression may be due to a bypass of the *cdc42-md* defects by the overexpressed kinases or to a restoration of a sufficiently effective interaction between the mutant Cdc42p and the kinases. In the latter model, the CRIB-binding defect of *cdc42-md2* causes a vegetative growth defect due to impaired interaction with Cla4p and a signaling defect due to impaired interactions with Ste20p.

Restoration of pheromone signaling in *cdc42-md* mutants by the *ste20ΔCRIB* allele. The findings presented above are consistent with the simple hypothesis that the Cdc42p-Ste20p interaction is a critical step in the α -factor signaling pathway: the *cdc42-md* mutants are defective for this interaction in vitro and in vivo; epistasis analysis suggests that Cdc42p acts at the same level of the pathway as Ste20p, and overexpression of Ste20p suppresses that the *cdc42-md* signaling defect. Nevertheless, the hypothesis that the Cdc42p-Ste20p interaction is important for signaling is contradicted by previous studies showing that a

ste20 mutant lacking the CRIB domain (and therefore defective in Cdc42p interaction) did not affect signaling (23, 37). A possible resolution of this apparent paradox is suggested by recent evidence that the CRIB domain in PAK family kinases is part of an autoinhibitory domain, leading to a model in which Cdc42p (or Rac) activates PAK family kinases by “relief of autoinhibition” (3, 49, 52, 54). For example, in the Pak1 kinase of *Schizosaccharomyces pombe*, a region overlapping the CRIB domain of Pak1 binds intramolecularly to the catalytic domain, yielding a “closed” conformation that can be “opened” either by binding to Cdc42p or by mutations in the CRIB domain (49). By analogy, the *ste20ΔCRIB* mutant may be competent for signal transduction because it no longer requires a normally critical interaction with Cdc42p for its activation. This hypothesis predicts that the *ste20ΔCRIB* mutant should bypass the requirement for Cdc42p in signaling, rendering *cdc42-md* strains sensitive to pheromone. Indeed, we found that *ste20ΔCRIB* restored significant α -factor signal-

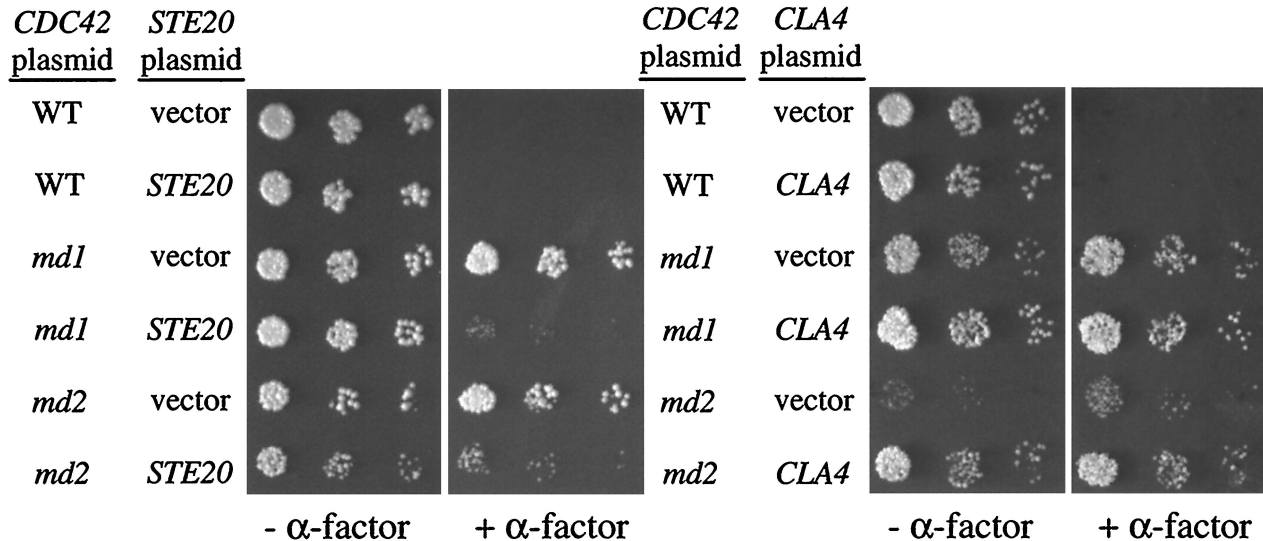


FIG. 8. Overexpression of *STE20* suppresses the *cdc42-md* signaling defect. Strain DLY3067 (*GAL1p-CDC42*) was transformed with pMOSB45 (wild type [WT]), pMOSB42 (*md1*), pMOSB43 (*md2*), or pMOSB44 (*md12*), and each strain was then transformed with pRS426 (vector), pVTU-*Ste20* (*STE20*), or pDLB722 (*CLA4*). The photographs show growth after 3 days at 23°C with (+) or without (-) α-factor.

ing to the *cdc42-md* mutants, as assayed by growth inhibition (Fig. 9A) or *FUS1* induction (Fig. 9B). This suggests that the *ste20ΔCRIB* allele encodes an activated form of Ste20p and supports the hypothesis that the Cdc42p-Ste20p interaction is normally important for pheromone signaling. We noticed, however, that *ste20ΔCRIB* did not completely restore α-factor sensitivity to *cdc42-md* mutants. This suggests that *cdc42-md* mutants have some defect in addition to the Ste20p activation defect.

Contribution of Bem1p to Cdc42p- and Ste20p-dependent signaling. The *BEM1* gene was discovered through its key role in polarity establishment (5, 9, 38). Subsequent studies showed that Bem1p can also modulate the pheromone response pathway, as Bem1p overexpression increases signaling while Bem1p removal decreases signaling (17, 29). Because the role of Bem1p in polarity establishment involves Cdc42p and Cdc24p (5, 38), we speculated that its role in pheromone-responsive signaling may also involve Cdc42p and therefore that the residual signaling defect observed in *cdc42-md* *ste20ΔCRIB* mutants might reflect reduced Bem1p function resulting from the *cdc42-md* mutations. Consistent with this hypothesis, we found that like *cdc42-md* *ste20ΔCRIB* mutants, *bem1Δ ste20ΔCRIB* mutants also displayed partial α-factor resistance (Fig. 10A) and reduced *FUS1* induction (Fig. 10B) compared to *ste20ΔCRIB* single mutants. The signaling defect in *bem1Δ ste20ΔCRIB* mutants was also evident when the pathway was activated by membrane-targeted Ste5p but not when it was activated by the activated Ste11p derivative Ste11ΔN (Fig. 10C). This indicates that like Cdc42p, Bem1p acts downstream of Ste5p membrane recruitment to promote activation of Ste11p by Ste20p.

We also compared the effects of *bem1Δ* and *ste20ΔCRIB* mutations on signaling by Ste5p that was targeted to different subcellular locations (Fig. 10D). Remarkably, while Ste20pΔCRIB was mildly defective at activating Ste5p that was targeted to the plasma membrane (Ste5ΔN-CTM), it showed increased ability to activate Ste5p that was targeted primarily to internal membranes (Ste5ΔN-Sec22 [40]). Consequently, in *ste20ΔCRIB* cells, the four- to fivefold signaling advantage of plasma membrane-targeted Ste5p over internal-membrane-targeted Ste5p was eliminated. These results support the notion that Ste20pΔCRIB is an active but delocalized kinase.

Loss of Bem1p did not mimic the effect of *ste20ΔCRIB*; instead, *bem1Δ* reduced the ability of Ste20pΔCRIB to support signaling by Ste5ΔN-Sec22 and Ste5ΔN-CTM to similar extents, indicating that Bem1p can affect Ste20p- and Ste5p-dependent signaling even when both components are mislocalized.

If a part of the signaling defect of *cdc42-md* mutants is due to defective Bem1p function, as argued above, then Bem1p overexpression might be expected to improve signaling in *cdc42-md* cells. Indeed, we found that a high-copy-number *BEM1* plasmid substantially improved signaling in response to membrane-targeted Ste5p in *cdc42-md1* and *cdc42-md2* mutant strains (Fig. 11). Bem1p overexpression also suppressed the growth and morphology defects of *cdc42-md* mutants (data not shown). However, this cannot account for the improved signaling because a high-copy-number *CLA4* plasmid (which also suppressed the growth and morphology defects) or introduction of both *cdc42-md1* and *cdc42-md2* (leading to complementation of the growth and morphology defects) failed to suppress the signaling defect (Fig. 11). Strikingly, Bem1p overexpression (but not Cla4p overexpression or *cdc42-md* combinations) also suppressed the Ste20p localization defect in *cdc42-md* mutants (Fig. 11). This result is consistent with previous studies indicating that Bem1p interacts with Ste20p (24) and strongly suggests that Bem1p is acting to promote signaling at the level of Ste20p, consistent with our epistasis results above. When combined, the introduction of Ste20pΔCRIB (to bypass the Ste20p activation defect) and excess Bem1p (to bypass a possible Bem1p defect) into the *cdc42-md1* mutant completely suppressed its α-factor resistance phenotype (Fig. 12). Together, these data suggest that the signaling defect of *cdc42-md* mutants can be accounted for by their simultaneous failures to activate Ste20p and to promote Bem1p function.

DISCUSSION

A role for Cdc42p in signal transduction in response to α-factor. We have isolated *cdc42* mutants that display recessive defects in α-factor signaling while retaining the ability to proliferate. All of these *cdc42-md* mutants had morphogenesis

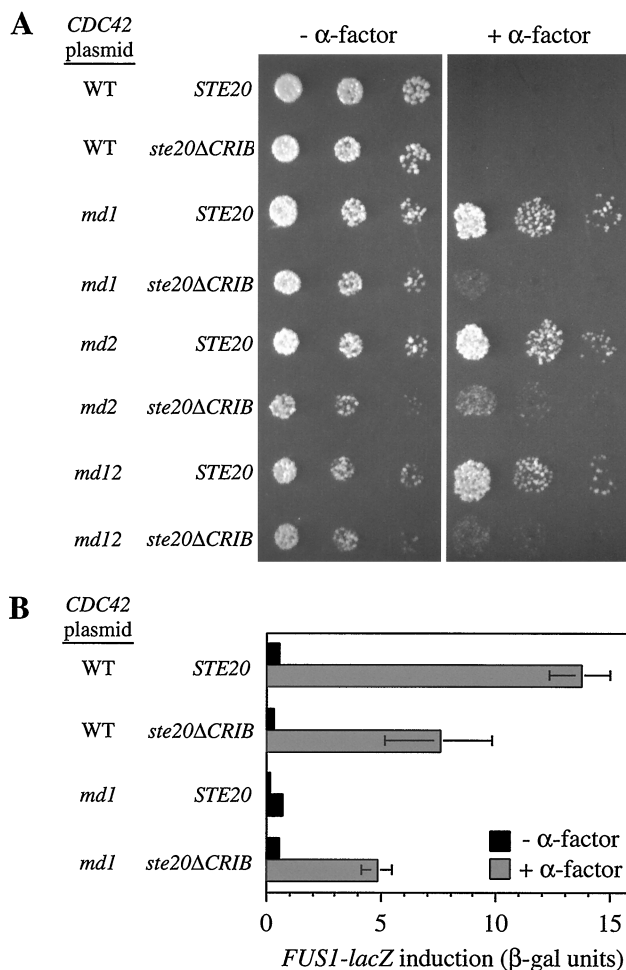


FIG. 9. *ste20ΔCRIB* largely restores α-factor sensitivity to *cdc42-md* strains. (A) Growth arrest. Strains DLY3067 (*GAL1p-CDC42 STE20*) and MOSY0268 (*GAL1p-CDC42 ste20ΔCRIB*) were transformed with pMOSB55 (wild type [WT]), pMOSB36 (*md1*), pMOSB37 (*md2*), or pMOSB38 (*md12*), as indicated. The photographs show growth after 3 days at 23°C with (+) or without (−) α-factor. (B) *FUS1-lacZ* induction. The same strains as in panel A harbored the *FUS1-lacZ* plasmid pSB231 plus either pMOSB45 (WT) or pMOSB42 (*md1*) and were assayed in glucose medium after 90 min with (+) or without (−) 0.01 μM α-factor. The bars indicate the means ± standard deviations of four transformants.

defects in addition to their signaling defect. However, the signaling defect is unlikely to be an indirect result of the morphogenesis defects for the following reasons. First, overexpression of *CLA4* suppressed the morphogenesis defects of *cdc42-md* mutants but not the signaling defect. Second, two pairwise combinations of *cdc42-md* alleles displayed intragenic complementation for their morphogenesis defects but not for their signaling defects. Third, a synchronous early-G₁-phase population of *cdc42-md1* mutant cells isolated by centrifugal elutriation displayed a signaling defect even during G₁ phase, a time when cells are uniformly sensitive to α-factor and Cdc42p-dependent polarity has yet to be established. It is difficult to see how a signaling defect in this synchronous culture could arise due to any indirect cell cycle or morphogenesis problems. In summary, these results strongly suggest that Cdc42p plays a role in α-factor-induced signaling that is separate from its roles in morphogenesis, confirming the sugges-

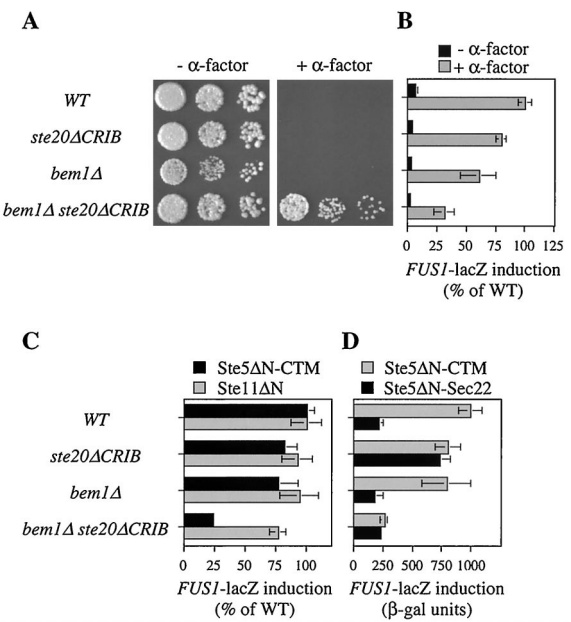


FIG. 10. *BEM1* is important for signaling in *ste20ΔCRIB* mutant strains. (A) Growth arrest. The photographs show growth after 2 days at 30°C with (+) and without (−) α-factor. (B) *FUS1-lacZ* induction by α-factor. Strains harboring a *FUS1-lacZ* reporter plasmid (p3058) were treated with and without 0.1 μM α-factor in duplicate for 1 and 2 h with similar results; the data were expressed as percent mean induced β-galactosidase activity in the wild-type (WT) strain (427 U at 1 h; 835 U at 2 h) and combined, with each bar representing the mean ± standard deviation (SD) of four measurements. (C) *FUS1-lacZ* induction by Ste5ΔN-CTM or Ste11ΔN was assayed in strains harboring p3058 and either pGFP-GS5ΔN-CTM or pGS11ΔN-T after 4 h of induction with galactose; the bars indicate the means ± SD of four to six transformants, expressed as percent mean induced β-galactosidase activity in the WT strain (1,024 U for Ste5ΔN-CTM; 644 U for Ste11ΔN). (D) *FUS1-lacZ* induction in strains harboring p3058 and either pGFP-GS5ΔN-CTM (Ste5ΔN-CTM) or pGFP-GS5ΔN-Sec22 (Ste5ΔN-Sec22) was assayed after 4 h of induction with galactose; the bars indicate the means ± SD of eight transformants. The strains in all panels were DLY1 (WT), MOSY0252 (*ste20ΔCRIB*), JMY1128 (*bem1Δ*), and MOSY0270 (*bem1Δ ste20ΔCRIB*).

tions from earlier studies with temperature-sensitive *cdc42* mutants (46, 47, 53).

The conclusion that Cdc42p is important for α-factor signaling is at odds with a study that found no signaling defect in G₁-arrested temperature-sensitive *cdc42* or *cdc24* mutants (35). In that study, cells arrested in G₁ by deprivation of G₁ cyclins were subsequently shifted to the restrictive temperature for the *cdc42* or *cdc24* mutants and then exposed to relatively high doses of α-factor. Under these conditions, induction of *FUS1* transcription was unaffected by the *cdc42* or *cdc24* mutations, suggesting that Cdc42p is not required for α-factor signaling and affects signaling indirectly as a result of cell cycle perturbation (35). However, an earlier study found Cdc24p and Cdc42p to be required for the maintenance of G₁ arrest in cells that had been prearrested by α-factor (46), which is not explainable by a model in which the signaling defects of *cdc24* and *cdc42* mutants are due simply to accumulation of cells at a nonresponsive stage of the cell cycle.

While our observations support a role for Cdc42p in pheromone-responsive signal transduction, they do not suggest that Cdc42p is a pathway intermediate that gets activated in response to pheromone. Instead, our work is consistent with the view (40) that Cdc42p plays a permissive role in maintaining cellular competence for signaling. For instance, Cdc42p may be constitutively required for the establishment of relatively long-lived pre-signaling complexes containing active Ste20p

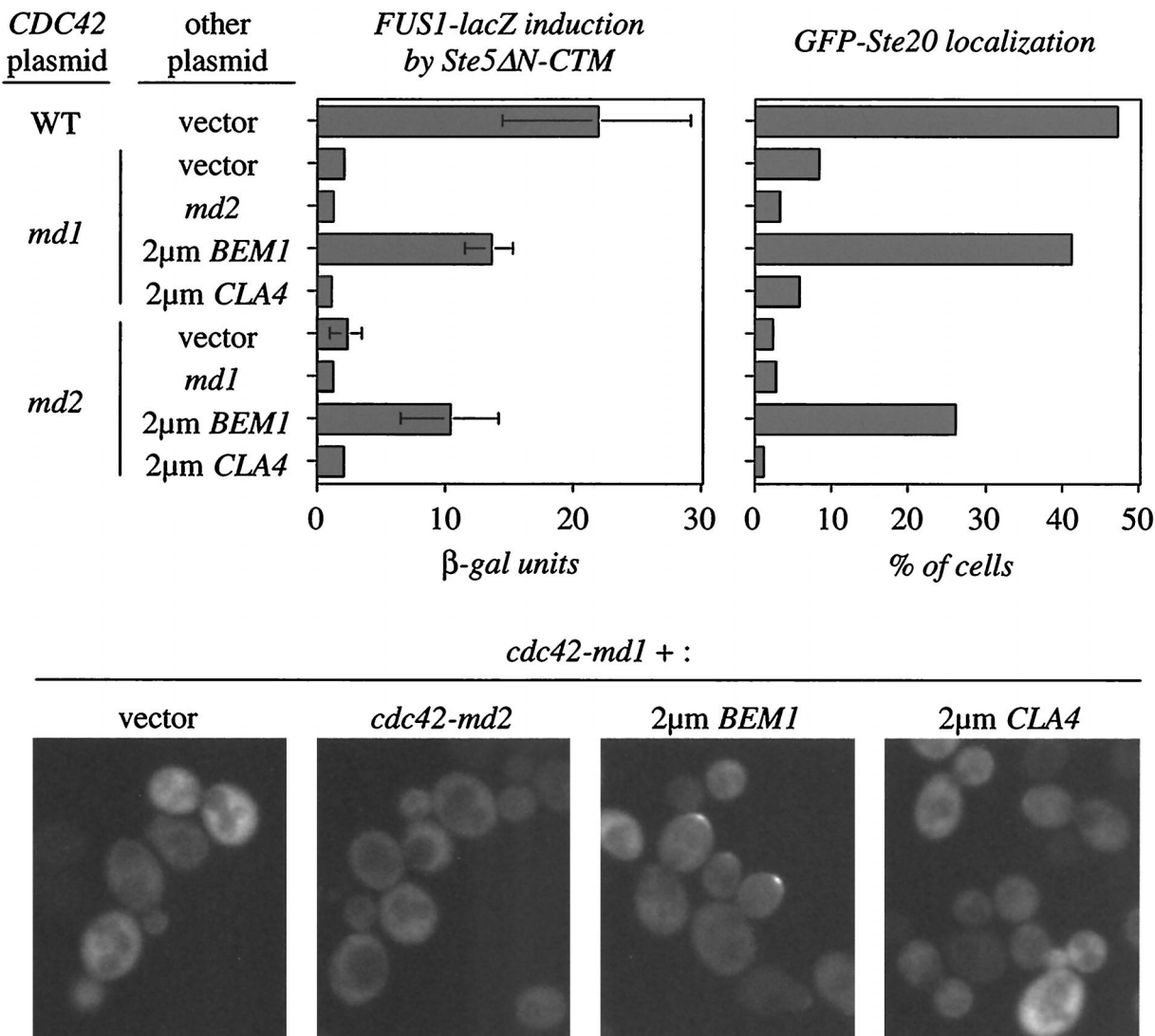


FIG. 11. Overproduction of *BEM1* restores Ste20p localization and signaling competence to *cdc42-md* strains. Strain PPY911 (*cdc42-1*) containing pL-GS5ΔN-CTM (for *FUS1* induction) or pPP828 (for Ste20p localization) was transformed with the *CDC42* plasmids pMOSB45 (wild type [WT]), pMOSB42 (*md1*), or pMOSB43 (*md2*) and then with YEpl24 (vector), pMOSB36 (*md1*), pMOSB37 (*md2*), pPB321 (2μm *BEM1*), or pDLB722 (2μm *CLA4*) as indicated. *FUS1-lacZ* induction was measured as for Fig. 4; the bars indicate means ± SD of six independent transformants. GFP-Ste20p localization was quantitated as for Fig. 7 (200 cells counted), and representative cells are shown below.

(see below). Transmission of the pheromone signal could then utilize this preactivated pool of Ste20p without any further immediate involvement of Cdc42p. In this hypothesis, the *cdc42-md* mutants have a signaling defect because they fail to establish this competent pool of Ste20p, while the temperature-sensitive *cdc42-1* inactivation regimen used by Oehlen and Cross (35) did not result in a signaling defect because sufficient Ste20p activation was established prior to the temperature shift to allow subsequent signaling. Notable in this regard is evidence from human PAK family members that GTPase-dependent establishment of the open conformation allows for PAK autophosphorylation, which subsequently interferes with regeneration of the closed conformation and thus makes the kinase temporarily GTPase independent (30, 52).

Ste20p is a key Cdc42p target involved in pheromone signaling. By several criteria, the *cdc42-md* mutants are defective in interacting with Ste20p: they are defective (to varying extents) in binding to the Ste20p CRIB domain in vitro, they fail

to localize Ste20p to bud tips in vivo, and they display synthetic lethality with *cla4* mutants. Furthermore, epistasis analysis suggests that *cdc42-md* mutants are defective in signal transduction at the same step in the pathway as *ste20* mutants (i.e., the activation of Ste11p following membrane targeting of Ste5p). Finally, the signaling defect of *cdc42-md* mutants is largely suppressed by overproduction of Ste20p. These data strongly support the hypothesis that the Cdc42p-Ste20p interaction is important for efficient signaling in the pheromone response pathway, as originally proposed (46, 53). However, more recent studies have argued that the Cdc42p-Ste20p interaction is dispensable for pheromone response, based on the signaling competence of a version of Ste20p (Ste20pΔCRIB) that cannot bind to Cdc42p. We found that Ste20pΔCRIB largely restored signaling competence to strains containing the *cdc42-md* mutants. This observation suggests that Ste20pΔCRIB is an activated version of Ste20p that no longer requires interaction with Cdc42p for its activation, consistent with current models for

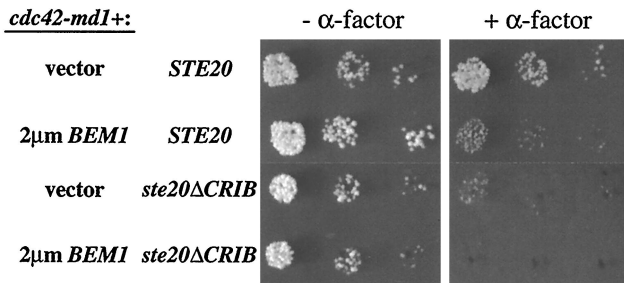


FIG. 12. Bem1p and Ste20pΔCRIB cooperate to restore α -factor sensitivity to a *cdc42-mdl* strain. Strains DLY3067 (*GAL1p-CDC42 STE20*) and MOSY0268 (*GAL1p-CDC42 ste20ΔCRIB*) were transformed with pMOSB42 (*cdc42-mdl*) and either pRS426 (vector) or pPB321 (2 μ m *BEM1*), as indicated. The photographs show growth after 3 days at 30°C with (+) and without (-) α -factor.

PAK activation which involve a relief of autoinhibition mechanism (3, 49, 54). We therefore conclude that interaction of Cdc42p with Ste20p is normally required for Ste20p to participate in the pheromone response pathway. Importantly, however, we do not find it necessary to propose that pheromone regulates either GTP loading of Cdc42p, the Cdc42p-Ste20p interaction, or Ste20p kinase activity. Instead, the simplest model consistent with available data is that access of Ste20p to its substrates is the pheromone-regulated step, with the effect of Cdc42p on Ste20p kinase activity being a preexisting condition that is independent of pheromone exposure (see reference 40 for further discussion).

Cdc42p may play a second role together with Bem1p in pheromone signaling. Although Ste20p appears to be the major Cdc42p target for signal transduction, our results suggest the existence of a second role for Cdc42p in this process, because *cdc42-mdl* mutants displayed a residual signaling defect even in the presence of the activated *ste20ΔCRIB* allele. Given the strong links between Cdc42p and the SH3-domain-containing scaffold protein Bem1p that have been established through studies of cell polarity in yeast (5, 9, 38), we suspected that this second role might involve Bem1p (which has also been shown to modulate the strength of α -factor signaling [17, 29]). Consistent with this hypothesis, Bem1p overexpression partially suppressed the signaling defect of *cdc42-mdl* mutants and Bem1p overexpression together with *ste20ΔCRIB* could fully suppress the α -factor-resistant growth of *cdc42-mdl* mutants.

Our observations suggest that the *cdc42-mdl* mutants are defective in activation of the Ste11p-Ste7p-Fus3p MAPK cascade. This step involves the interaction of G β γ with the Ste5p scaffold protein (associated with Ste11p, Ste7p, and Fus3p), resulting in recruitment of Ste5p to the plasma membrane (40) and also the interaction of G β γ with Ste20p (25). These interactions likely serve to raise the local concentrations of Ste20p and its substrate Ste11p (bound to Ste5p), thereby initiating MAPK cascade activity. The previously described effects of Bem1p on pheromone signaling (20, 29) are compatible with its acting anywhere in the pathway from receptor to the MAPK Fus3p. Our experiments indicate that Bem1p affects steps following Ste5p membrane recruitment, since both loss and overproduction of Bem1p affects signaling by membrane-targeted Ste5p, even in cells with the activated *ste20ΔCRIB* allele. In contrast, signaling by the activated Ste11p derivative Ste11 Δ N was comparatively insensitive to the loss of Bem1p. We also observed that Bem1p can affect the localization of Ste20p, and previous studies showed that Bem1p could form complexes with both Ste20p and Ste5p (24, 29). Together, these results

suggest that Bem1p influences activation of the Ste5p-associated kinase cascade by Ste20p, perhaps by helping to bring these proteins together. It should be noted that earlier work observed effects of Bem1p overproduction on the residual pheromone response of *ste20Δ* cells (20, 29); the mechanism for this residual response has not been determined, but it may rely on inefficient substitution for Ste20p by another PAK family kinase (e.g., Cla4p), which would be compatible with our suggestion that Bem1p affects the step in which Ste11p is activated by the Ste20p (or substitute) kinase.

The dramatic effect of Bem1p overexpression on Ste20p localization in *cdc42-mdl* mutants provides a suggestion as to how Bem1p may function. During vegetative growth, recruitment of Ste20p to the bud tip by Cdc42p may be assisted by Bem1p-mediated local retention of Ste20p. Similarly, during pheromone response, recruitment of Ste5p and Ste20p to a region of the plasma membrane by G β γ may be assisted by local retention of these proteins promoted by Bem1p. Our results suggest some collaboration between Cdc42p and Bem1p in pheromone response. Thus, Cdc42p and Bem1p may each help to provide a cell surface scaffold that facilitates the association and/or local retention of Ste5p (with its associated kinases) and Ste20p, allowing the local concentrations of these signaling components to be raised above the threshold required for efficient signal transduction.

Conclusions. In aggregate, the analysis of the pheromone-resistant *cdc42* alleles presented here combined with previous studies suggest a novel paradigm for the “signaling” role of Cdc42p that is quite distinct from the paradigm established for the ras GTPase. Cdc42p is required for Ste20p activation, but there is little evidence to suggest that pheromone signals stimulate this activation; instead, pheromone signaling may make use of a preexisting constitutive Ste20p activity. In addition, Cdc42p (acting with Bem1p) helps increase the local concentration of Ste20p together with other signaling components, promoting signal transduction by a proximity effect (36). Providing a surface conducive to the local concentration of signaling reactants could be a common contributor to eukaryotic signaling pathways, especially those that rely on regulatable protein-protein interactions rather than diffusible second messengers (16). It remains to be seen to what extent these types of signaling roles will be generally applicable for other Rho family GTPases and other cells.

ACKNOWLEDGMENTS

We thank members of the Pringle and Lew laboratories for many valuable discussions. We also thank E. Bi, C. Boone, F. Cross, E. Leberer, and M. Peter for providing plasmids or strains. Thanks to Lynn Martinek and Mike Cook from the Duke Cancer Center Flow Cytometry Shared Resource for help with the flow cytometry.

J.J.M. was supported by American Cancer Society postdoctoral fellowship PF-98-008. This work was supported by grants from the Worcester Foundation and the Millipore Foundation, by NIH grant GM57769 to P.M.P., and by NIH grant GM53050 and American Cancer Society grant RPG-98-046-CCG to D.J.L.

REFERENCES

- Adams, A. E. M., D. I. Johnson, R. M. Longnecker, B. F. Sloat, and J. R. Pringle. 1990. *CDC42* and *CDC43*, two additional genes involved in budding and the establishment of cell polarity in the yeast *Saccharomyces cerevisiae*. *J. Cell Biol.* **111**:131–142.
- Ausubel, F. M., R. Brent, R. E. Kingston, D. D. Moore, J. G. Seidman, J. A. Smith, and K. Struhl (ed.). 1995. Current protocols in molecular biology. John Wiley and Sons, New York, N.Y.
- Bagrodia, S., and R. A. Cerione. 1999. Pak to the future. *Trends Cell Biol.* **9**:350–355.
- Bardwell, L., J. G. Cook, C. J. Inouye, and J. Thorner. 1994. Signal propagation and regulation in the mating pheromone response pathway of the yeast *Saccharomyces cerevisiae*. *Dev. Biol.* **166**:363–379.

5. Bender, A., and J. R. Pringle. 1991. Use of a screen for synthetic lethal and multicopy suppressor mutants to identify two new genes involved in morphogenesis in *Saccharomyces cerevisiae*. *Mol. Cell. Biol.* **11**:1295–1305.
6. Benton, B. K., A. Tinklenberg, I. Gonzalez, and F. R. Cross. 1997. Cla4p, a *Saccharomyces cerevisiae* Cdc42p-activated kinase involved in cytokinesis, is activated at mitosis. *Mol. Cell. Biol.* **17**:5067–5076.
7. Boeke, J. D., J. Trueheart, G. Natsoulis, and G. R. Fink. 1987. 5-Fluoroorotic acid as a selective agent in yeast molecular genetics. *Methods Enzymol.* **154**:164–173.
8. Burbelo, P. D., D. Drechsel, and A. Hall. 1995. A conserved binding motif defines numerous candidate target proteins for both Cdc42 and Rac GTPases. *J. Biol. Chem.* **270**:29071–29074.
9. Chenevert, J., K. Corrado, A. Bender, J. Pringle, and I. Herskowitz. 1992. A yeast gene (*BEM1*) necessary for cell polarization whose product contains two SH3 domains. *Nature* **356**:77–79.
10. Elder, R. T., E. Y. Loh, and R. W. Davis. 1983. RNA from the yeast transposable element Ty1 has both ends in the direct repeats, a structure similar to retrovirus RNA. *Proc. Natl. Acad. Sci. USA* **80**:2432–2436.
11. Feng, Y., L. Y. Song, E. Kincaid, S. K. Mahanty, and E. A. Elion. 1998. Functional binding between Gβ and the LIM domain of Ste5 is required to activate the MEKK1Ste11. *Curr. Biol.* **8**:267–278.
12. Gietz, R. D., and A. Sugino. 1988. New yeast-*Escherichia coli* shuttle vectors constructed with in vitro mutagenized yeast genes lacking six base pair restriction sites. *Gene* **74**:527–534.
13. Guthrie, C., and G. R. Fink (ed.). 1991. Methods in enzymology, vol. 194. Guide to yeast genetics and molecular biology. Academic Press, Inc., San Diego, Calif.
14. Haase, S. B., and D. J. Lew. 1997. Flow cytometric analysis of DNA content in budding yeast. *Methods Enzymol.* **283**:322–332.
15. Hudson, J. R., Jr., E. P. Dawson, K. L. Rushing, C. H. Jackson, D. Lockshon, D. Conover, C. Lanciault, J. R. Harris, S. J. Simmons, R. Rothstein, and S. Fields. 1997. The complete set of predicted genes from *Saccharomyces cerevisiae* in a readily usable form. *Genome Res.* **7**:1169–1173.
16. Hunter, T. 2000. Signaling—2000 and beyond. *Cell* **100**:113–127.
17. Kao, L. R., J. Peterson, R. Ji, L. Bender, and A. Bender. 1996. Interactions between the ankyrin repeat-containing protein Akr1p and the pheromone response pathway in *Saccharomyces cerevisiae*. *Mol. Cell. Biol.* **16**:168–178.
18. Kozminski, K. G., A. J. Chen, A. A. Rodal, and D. G. Drubin. 2000. Functions and functional domains of the GTPase Cdc42p. *Mol. Biol. Cell.* **11**:339–354.
19. Lamarche, N., N. Tapon, L. Stowers, P. D. Burbelo, P. Aspenstrom, T. Bridges, J. Chant, and A. Hall. 1996. Rac and Cdc42 induce actin polymerization and G1 cell cycle progression independently of p65PAK and the JNK/SAPK MAP kinase cascade. *Cell* **87**:519–529.
20. Leberer, E., J. Chenevert, T. Leeuw, D. Harcus, I. Herskowitz, and D. Y. Thomas. 1996. Genetic interactions indicate a role for Mdg1p and the SH3 domain protein Bem1p in linking the G-protein mediated yeast pheromone signalling pathway to regulators of cell polarity. *Mol. Gen. Genet.* **252**:608–621.
21. Leberer, E., D. Dignard, D. Harcus, D. Y. Thomas, and M. Whiteway. 1992. The protein kinase homologue Ste20p is required to link the yeast pheromone response G-protein βγ subunits to downstream signaling components. *EMBO J.* **11**:4815–4824.
22. Leberer, E., D. Y. Thomas, and M. Whiteway. 1997. Pheromone signalling and polarized morphogenesis in yeast. *Curr. Opin. Genet. Dev.* **7**:59–66.
23. Leberer, E., C. Wu, T. Leeuw, A. Fourest-Lievin, J. E. Segall, and D. Y. Thomas. 1997. Functional characterization of the Cdc42p binding domain of yeast Ste20p protein kinase. *EMBO J.* **16**:83–97.
24. Leeuw, T., A. Fourest-Lievin, C. Wu, J. Chenevert, K. Clark, M. Whiteway, D. Y. Thomas, and E. Leberer. 1995. Pheromone response in yeast: association of Bem1p with proteins of the MAP kinase cascade and actin. *Science* **270**:1210–1213.
25. Leeuw, T., C. Wu, J. D. Schrag, M. Whiteway, D. Y. Thomas, and E. Leberer. 1998. Interaction of a G-protein β-subunit with a conserved sequence in Ste20/PAK family protein kinases. *Nature* **391**:191–195.
26. Lew, D. J., and S. I. Reed. 1995. A cell cycle checkpoint monitors cell morphogenesis in budding yeast. *J. Cell Biol.* **129**:739–749.
27. Lew, D. J., and S. I. Reed. 1993. Morphogenesis in the yeast cell cycle: regulation by Cdc28 and cyclins. *J. Cell Biol.* **120**:1305–1320.
28. Liu, Q., M. Z. Li, D. Leibham, D. Cortez, and S. J. Elledge. 1998. The univector plasmid-fusion system, a method for rapid construction of recombinant DNA without restriction enzymes. *Curr. Biol.* **8**:1300–1309.
29. Lyons, D. M., S. K. Mahanty, K. Y. Choi, M. Manandhar, and E. A. Elion. 1996. The SH3-domain protein Bem1 coordinates mitogen-activated protein kinase cascade activation with cell cycle control in *Saccharomyces cerevisiae*. *Mol. Cell. Biol.* **16**:4095–4106.
30. Martin, G. A., G. Bollag, F. McCormick, and A. Abo. 1995. A novel serine kinase activated by rac1/CDC42Hs-dependent autop phosphorylation is related to PAK65 and STE20. *EMBO J.* **14**:1970–1978. (Erratum, **14**:4385.)
31. Mosch, H. U., R. L. Roberts, and G. R. Fink. 1996. Ras2 signals via the Cdc42/Ste20/mitogen-activated protein kinase module to induce filamentous growth in *Saccharomyces cerevisiae*. *Proc. Natl. Acad. Sci. USA* **93**:5352–5356.
32. Neiman, A. M., and I. Herskowitz. 1994. Reconstitution of a yeast protein kinase cascade in vitro: activation of the yeast MEK homologue STE7 by STE11. *Proc. Natl. Acad. Sci. USA* **91**:3398–3402.
33. Nern, A., and R. A. Arkowitz. 1998. A GTP-exchange factor required for cell orientation. *Nature* **391**:195–198.
34. Oehlen, L. J. W. M., and F. R. Cross. 1994. G1 cyclins CLN1 and CLN2 repress the mating factor response pathway at Start in the yeast cell cycle. *Genes Dev.* **8**:1058–1070.
35. Oehlen, L. J. W. M., and F. R. Cross. 1998. The role of Cdc42 in signal transduction and mating of the budding yeast *Saccharomyces cerevisiae*. *J. Biol. Chem.* **273**:8556–8559.
36. Pawson, T., and J. D. Scott. 1997. Signaling through scaffold, anchoring, and adaptor proteins. *Science* **278**:2075–2080.
37. Peter, M., A. M. Neiman, H.-O. Park, M. van Lohuizen, and I. Herskowitz. 1996. Functional analysis of the interaction between the small GTP binding protein Cdc42 and the Ste20 protein kinase in yeast. *EMBO J.* **15**:7046–7059.
38. Pringle, J. R., E. Bi, H. A. Harkins, J. E. Zahner, C. De Virgilio, J. Chant, K. Corrado, and H. Fares. 1995. Establishment of cell polarity in yeast. *Cold Spring Harbor Symp. Quant. Biol.* **60**:729–744.
39. Pryciak, P. M., and L. H. Hartwell. 1996. *AKR1* encodes a candidate effector of the βγ complex in the *Saccharomyces cerevisiae* pheromone response pathway and contributes to control of both cell shape and signal transduction. *Mol. Cell. Biol.* **16**:2614–2626.
40. Pryciak, P. M., and F. A. Huntress. 1998. Membrane recruitment of the kinase cascade scaffold protein Ste5 by the βγ complex underlies activation of the yeast pheromone response pathway. *Genes Dev.* **12**:2684–2697.
41. Reed, S. I., J. Ferguson, and J. Groppe. 1982. Preliminary characterization of the transcriptional and translational products of the *Saccharomyces cerevisiae* cell division cycle gene *CDC28*. *Mol. Cell. Biol.* **2**:415–425.
- 41a. Richardson, H. E., C. Wittenberg, F. Cross, and S. I. Reed. 1989. An essential G1 function for cyclin-like proteins in yeast. *Cell* **59**:1127–1133.
42. Sambrook, J., E. F. Fritsch, and T. Maniatis. 1989. Molecular cloning: a laboratory manual, 2nd ed. Cold Spring Harbor Laboratory Press, Cold Spring Harbor, NY.
43. Schild, D., A. J. Brake, M. C. Kiefer, D. Young, and P. J. Barr. 1990. Cloning of three multifunctional de novo purine biosynthetic genes by functional complementation of yeast mutants. *Proc. Natl. Acad. Sci. USA* **87**:2916–2920.
44. Shinjo, K., K. G. Koland, M. J. Hart, V. Narasimhan, D. I. Johnson, T. Evans, and R. A. Cerione. 1990. Molecular cloning of the gene for the human placental GTP-binding protein Gp (G25K): identification of this GTP-binding protein as the human homolog of the yeast cell-division cycle protein CDC42. *Proc. Natl. Acad. Sci. USA* **87**:9853–9857.
45. Sikorski, R. S., and P. Hieter. 1989. A system of shuttle vectors and yeast host strains designed for efficient manipulation of DNA in *Saccharomyces cerevisiae*. *Genetics* **122**:19–27.
46. Simon, M. N., C. De Virgilio, B. Souza, J. R. Pringle, A. Abo, and S. I. Reed. 1995. Role for the Rho-family GTPase Cdc42 in yeast mating-pheromone signal pathway. *Nature* **376**:702–705.
47. Stevenson, B. J., B. Ferguson, C. De Virgilio, E. Bi, J. R. Pringle, G. Ammerer, and G. F. Sprague, Jr. 1995. Mutation of *RGA1*, which encodes a putative GTPase-activating protein for the polarity-establishment protein Cdc42p, activates the pheromone-response pathway in the yeast *Saccharomyces cerevisiae*. *Genes Dev.* **9**:2949–2963.
48. Trueheart, J., J. Boeke, and G. R. Fink. 1987. Two genes required for cell fusion during yeast conjugation: evidence for a pheromone-induced surface protein. *Mol. Cell. Biol.* **7**:2316–2328.
49. Tu, H., and M. Wigler. 1999. Genetic evidence for Pak1 autoinhibition and its release by Cdc42. *Mol. Cell. Biol.* **19**:602–611.
50. Whiteway, M., L. Hougan, and D. Y. Thomas. 1990. Overexpression of the *STE4* gene leads to mating response in haploid *Saccharomyces cerevisiae*. *Mol. Cell. Biol.* **10**:217–222.
51. Whiteway, M. S., C. Wu, T. Leeuw, K. Clark, A. Fourest-Lievin, D. Y. Thomas, and E. Leberer. 1995. Association of the yeast pheromone response G protein βγ subunits with the MAP kinase scaffold Ste5p. *Science* **269**:1572–1575.
52. Zenke, F. T., C. C. King, B. P. Bohl, and G. M. Bokoch. 1999. Identification of a central phosphorylation site in p21-activated kinase regulating autoinhibition and kinase activity. *J. Biol. Chem.* **274**:32565–32573.
53. Zhao, Z. S., T. Leung, E. Manser, and L. Lim. 1995. Pheromone signalling in *Saccharomyces cerevisiae* requires the small GTP-binding protein Cdc42p and its activator Cdc24p. *Mol. Cell. Biol.* **15**:5246–5257.
54. Zhao, Z. S., E. Manser, X. Q. Chen, C. Chong, T. Leung, and L. Lim. 1998. A conserved negative regulatory region in alphaPAK: inhibition of PAK kinases reveals their morphological roles downstream of Cdc42 and Rac1. *Mol. Cell. Biol.* **18**:2153–2163.
55. Ziman, M., J. M. O'Brien, L. A. Ouellette, W. R. Church, and D. I. Johnson. 1991. Mutational analysis of *CDC42Sc*, a *Saccharomyces cerevisiae* gene that encodes a putative GTP-binding protein involved in the control of cell polarity. *Mol. Cell. Biol.* **11**:3537–3544.